

# Renewable energy resources in Mali - preliminary mapping

**Nygaard, Ivan; Badger, Jake; Larsen, Søren Ejling; Rasmussen, Kjeld; Nielsen, Thomas Theis; Hansen, Lars Boye; Mariko, Adama; Togola, Ibrahim**

*Publication date:*
2008

*Document Version*
Publisher's PDF, also known as Version of record

Risø National Laboratory for Sustainable Energy
Technical University of Denmark, Roskilde, Denmark

# Renewable energy resources in Mali – preliminary mapping

Final report, June 2008

Danida Contract: FK 2007/287/2

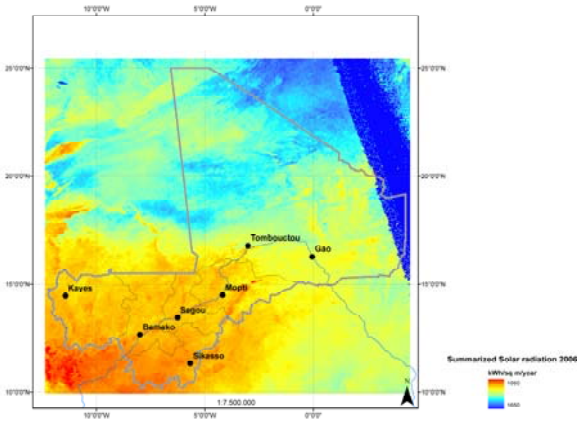


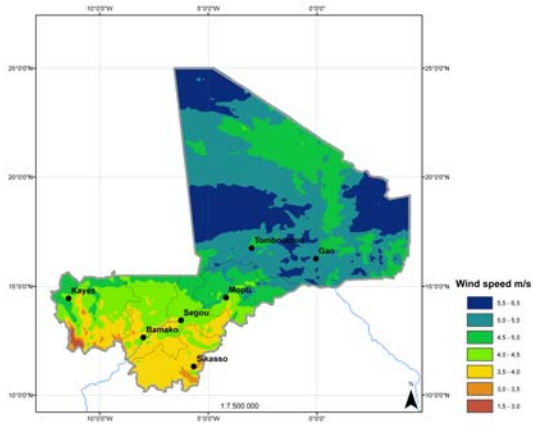


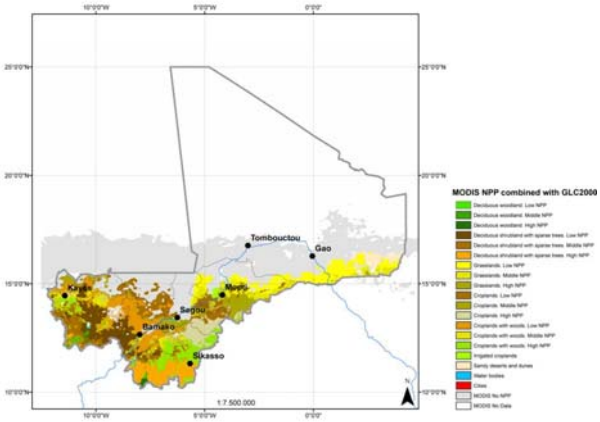


DEPARTMENT OF GEOGRAPHY & GEOLOGY
UNIVERSITY OF COPENHAGEN

Authors: Jake Badger, Søren Larsen, Kjeld Rasmussen, Thomas Theis Nielsen, Lars Boye Hansen, Adama Mariko, Ibrahim Togola

June 2007

Title: Renewable energy resources in Mali – preliminary mapping

**Contract no.:**

Danida FK 2007/287/2

**Editor: Ivan Nygaard**

UNEP Risoe Centre
Risø National Laboratory
Technical University of Denmark
P.O.Box 49
DK-4000 Roskilde
Denmark
Telephone +45 46775115
ivan.nygaard@risoe.dk
www.risoe.dtu.dk

# Contents

# List of abbreviations

| | |
|---|---|
| CNESOLER | Centre National de l'Energie Solaire et des Energies Renouvelables |
| CoV | Coefficient of Variance |
| DGG | Department of Geography and Geology |
| DNE | Direction Nationale de l'Energie |
| ENI | Ècole Nationale d'Ingenieurs |
| FAO | Food and Agriculture Organization |
| GIMMS | Global Inventory Modeling and Mapping Studies |
| GTZ | Deutsche Gesellschaft für Technische Zusammenarbeit |
| IFNS | Inverse Froude Number Squared |
| iNDVI | integrated NDVI |
| IPCC | Intergovermental Panel on Climate Change |
| ITCZ | Intertropical Convergence Zone |
| KAMM | Karlsruhe Atmospheric Mesoscale Model |
| MMEE | Ministère des Mines, de l'Energie et de l'Eau |
| MSG | Meterosat Second Generation |
| NASA | National (USA) Aeronautics and Space Administration |
| NCAR | National (USA) Center for Atmospheric Research |
| NCEP | National (USA) Center for Environmental Prediction |
| NDVI | Normalized Difference Vegetation Index |
| NGA | National (USA) Geospatial-Intelligence Agency |
| NIR | Refers to the surface's reflectance factor |
| NPP | Net Primary Productivity (Productivité Primaire Nette) |
| RED | Refers to the surface's reflectance factor in the red part of the spectrum. |
| RMSE | Root Mean Square Error |
| SRTM | Shuttle Radar Topography Mission |
| SSE | Surface meteorology and Solar Energy |
| TERNA | Technical Expertise for Renewable Energy Application |
| USGS | United States Geological Survey |
| UTM | Universal Transverse Mercator coordinate system |
| WAsP | Wind Atlas Analysis and Application Program |

# 1 Preface

The energy supply for households in Mali has traditionally been based on wood fuel and charcoal. In recent decades electrification of major towns has been progressing. Parts of Mali are connected by a national grid, and most of the energy derives from hydro-power, not the least from the Manantali Dam in the western part of Mali. In addition, a number of isolated grids, supplying power to limited, mostly urban, areas, exist, fuelled mainly by diesel. The energy demand of the transport sector has been based on imported diesel and gasoline as well.

Mali has since the 1980s, in cooperation with a various development partners conducted a number of development projects and programs focusing on increased use of renewable energy sources, and the Ministry for Mines, Energy and Water has developed a strategy for development of renewable energy in Mali, which was adopted by the Ministerial council (Conseil des Ministres) the 26 of December 2006. (MMEE, 2007). This strategy combines the efforts of reducing poverty, validation of national energy resources and ensuring long-term security and environmental sustainability of the energy supply. Given the rapid increase of prices on imported fuels, such as diesel and gasoline, it is increasingly worthwhile assessing the potential for giving renewable energy resources a central role in the future energy system: Environmentally friendly renewable energy resources are abundant in Mali and they are becoming increasingly competitive.

This technical report is the result of a first phase of a study financed by the Danish National Development Cooperation, Danida under the heading 'Provisional mapping of Renewable Energy Resources in Mali. 'Carte provisoire de ressources renouvelables du Mali')

The project reported here has as its objective to produce a national-scale mapping of (some of) these resources, by use of data derived from satellite images and models. The purpose is to provide tools useful to energy planners, wishing to assess the potential for producing wind power, solar power and biomass energy in Mali. Not all renewable energy resources are mapped, however. The most important exception is the stock of energy-resources contained in Mali's woody vegetation, which is not easily assessed from satellite data, and which is being assessed by other ongoing projects.

Wind resources are represented in a preliminary wind atlas, derived only from output from meteorological models along with information on terrain and land cover (and its associated surface roughness). In the next phase of the project this will be calibrated, validated and refined by use of mast measurements of wind. Solar energy resources are also represented in maps, based only on the use of Meteosat Second Generation (MSG) satellite data. Also for solar energy, ground measurements will be available for the second phase of the project, and they will be used for calibration and validation of the maps.

It is far more difficult to produce useful assessments of the biomass resources available for energy purposes. This is due to the following: (1) the energy contained in the 'standing biomass' is not a measure of the 'sustainable yield' of biomass energy. (2) The 'net primary productivity' (NPP), which may be the best proxy of this 'sustainable yield', is not of a fixed size, since human manipulation of it, e.g. in the form of irrigation or inputs of fertilizer, may increase it, and since human overuse of it, e.g. in the form of overgrazing of excessive felling of trees, may cause

it to decline. (3) The NPP may be harvested for human consumption, grazed by livestock (or wild animals) or burnt, and thus only some minor and variable fraction may be available for energy uses. (4) The spatial and temporal variability of the availability of bio-energy is great, and the coarse resolution satellite data, used to carry out national scale mapping, may not suffice to identify even important concentrations of resources. Therefore, the assessment of biomass resources includes at national-scale rough assessment of NPP, supplemented with an identification of some potentially interesting, specific bio-energy resources, which will require further in-depth studies, planned for the subsequent phase of the project.

The present project is carried out by Risø-DTU with the Department of Geography and Geology (DGG), University of Copenhagen, Ècole Nationale d'Ingenieurs (ENI), and Mali Folkecenter Nyata as subcontractors. The project is conducted in close cooperation with Direction Nationale de l'Energie (DNE) and Centre National de l'Energie Solaire et des Energies Renouvelables (CNESOLER), Mali.

The authors of chapter 1 are Jake Badger and Søren Larsen from Risø-DTU. Authors of chapter 2 and 3 are Kjeld Rasmussen and Thomas Theis Nielsen from DGG, Lars Boye Hansen, GRAS A/S (as a consultant to DGG) and Adama Mariko, ENI, Bamako. Ibrahim Togola is the author of appendix B

The project has been managed by Ivan Nygaard, Risø-DTU, who has also been responsible for editing the final report.

# 2 Wind assessment

## 2.1 Introduction

The conventional method used to produce estimates of wind resource over large areas or regions, such as on a national scale, is to analyze wind measurements made at a number of sites around the region, as in for example the European Wind Atlas (Troen and Petersen, 1989). In order for this method to work well there needs to be a sufficient quantity of high quality data, covering the country. This criterion is sometimes difficult to satisfy and therefore other methods are required – methods that will not meet bankable accuracy in resource estimates, but on the other hand will typically give good indications of the geographical distribution of the wind resource, and as such will be very useful for decision making and planning of feasibility studies.

**Numerical wind atlas** methodologies have been devised to solve the issue of insufficient wind measurements. One such methodology is the KAMM/WAsP method developed at Risø National Laboratory (Frank and Landberg, 1997).

In this methodology an approach called **statistical-dynamical downscaling** is used (Frey-Buness et al, 1995). The basis for the method is that there is a robust relationship between meteorological situations at the large-scale and meteorological situations at the small-scale.

Information about the large-scale meteorological situation is freely available from the NCEP/NCAR reanalysis data-set, Kalnay et al (1996). This data-set has been created by assimilating measurement data from around the globe in a consistent fashion from 1948 to the present day. The primary purpose for the generation of this data-set is to provide a reference for the state of the atmosphere and to identify any features of climate change. Another application of the data-set is as a long-term record of large-scale wind conditions. The NCEP/NCAR data is used to create around 100 different large-scale wind situations, called wind classes that represent the large-scale wind climate.

In order to make these wind classes meaningful at a smaller scale a mesoscale model is used to find out how the large-scale wind forcing is modified by regional scale topography. Therefore for each wind class a mesoscale model simulation is performed using the Karlsruhe Atmospheric Mesoscale Model (KAMM, Adrian and Fiedler, 1991).

Post-processing of the results from all the simulations yields a wind resource map at the resolution of the model simulations. Further analysis of the results from the simulations with consideration to the topography as described in the mesoscale model, yields wind atlas maps for generalized surface conditions. Files containing detailed information about the wind speed and direction distributions that are directly compatible with the WAsP software (Mortensen et al, 2007), the wind industry standard for site resource assessment calculations, can also be generated.

## 2.2 Model Description

The Karlsruhe Atmospheric Mesoscale Model (KAMM) is a 3D, non-hydrostatic, and incompressible mesoscale model. It is described in Adrian and Fiedler (1991), and Adrian (1994). Spatial derivatives are calculated in the model by central differences on a terrain following grid. The turbulent fluxes are modelled using a mixing-length model with stability dependent turbulent diffusion coefficients in stably stratified flow, and a non-local closure for the convective mixed layer. Lateral boundary conditions assume zero gradients normal to the inflow sides. On outflow boundaries, the horizontal equations of motion are replaced by a simple wave equation allowing signals to propagate out of the domain without reflection. Gravity waves can penetrate the upper boundary outward using the boundary condition of Klemp and Durran (1983).

KAMM is able to run as a "stand-alone" model, i.e. the model can be run by using only the large-scale forcing in the form of a single vertical profile of geostrophic wind and virtual potential temperature. Hence, it is not necessary to nest the mesoscale model within a larger model that must supply the boundary conditions. At regional scales the mesoscale model is used to model atmospheric flows in domains of 100-1000 km x 100-1000 km in size with a typical horizontal resolution of 2.5 to 10 km.

In the vertical the model extends from sea level to 5500 m above sea level, using 25 model levels employing a terrain following coordinate system. The interval between vertical levels is not uniform. This allows for more closely spaced vertical model levels near to terrain. The first 5 model levels are at 0 m, 20.3 m, 58.7 m, 115.3 m and 190.0 m above the surface. The separation between these levels is smaller in elevated terrain.

Figure 1.1 shows terrain elevation for the modelling domains used for this numerical wind atlas study. The surface elevation data is derived from NASA's Shuttle Radar Topography Mission (STRM30) dataset version 2. The dataset can be accessed via the USA's National Aeronautics and Space Administration (NASA) webpage (Internet Link [1]). This data uses a longitude-latitude projection at 30 arc second resolution. This elevation data is manipulated first to change it to a UTM coordinate system and then to change the coordinate system and resolution appropriately for the mesoscale simulations.

The aerodynamic surface roughness length data is derived from the United States Geological Survey (USGS) Global Land Cover Classification, also known as GLCC. The data can be accessed via a USGS webpage (Internet Link [2]). By means of a look-up table, the land-use types were converted to aerodynamic surface roughness lengths. This roughness data is manipulated first to change it to a UTM coordinate system and then to change the coordinate system and resolution appropriately for the mesoscale simulations. The map of the surface roughness for the mesoscale modelling domains is shown in Figure 2.2.

(a)

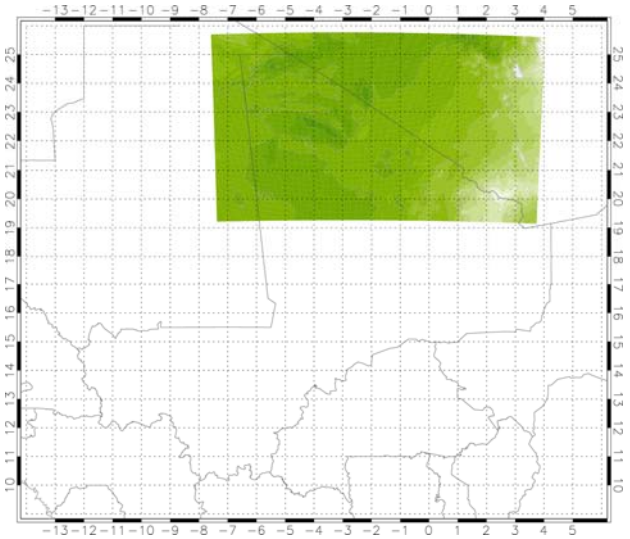

(b)

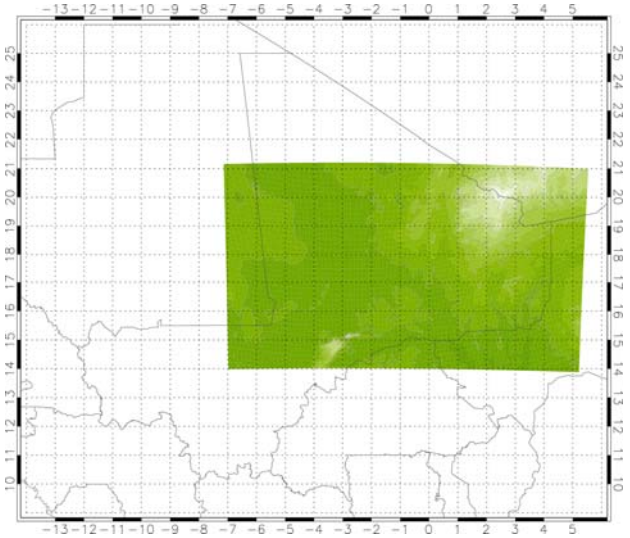

(c)

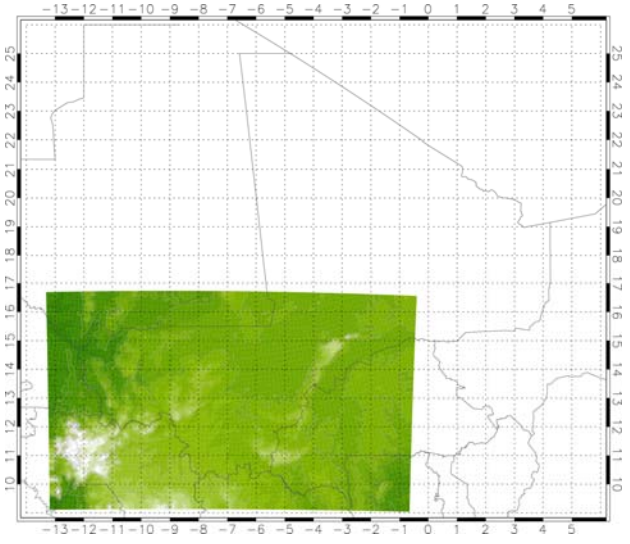

*Figure 2.1: The surface elevation over the three computational domains used for the KAMM mesoscale modelling at 7.5 km resolution; (a) Northern Mali, (b) Central Mali, (c) Southern Mali. The contour interval is 100 m. The x and y axis are in longitude and latitude. The data is derived from NASA's Shuttle Radar Topography Mission (STRM) dataset version 2.*

(a)

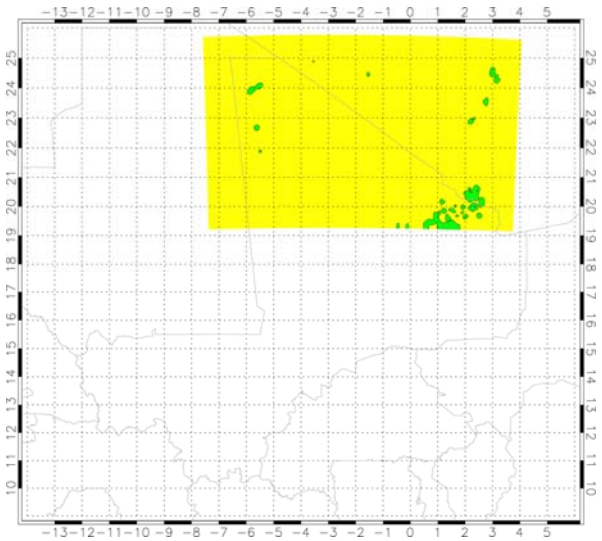

(b)

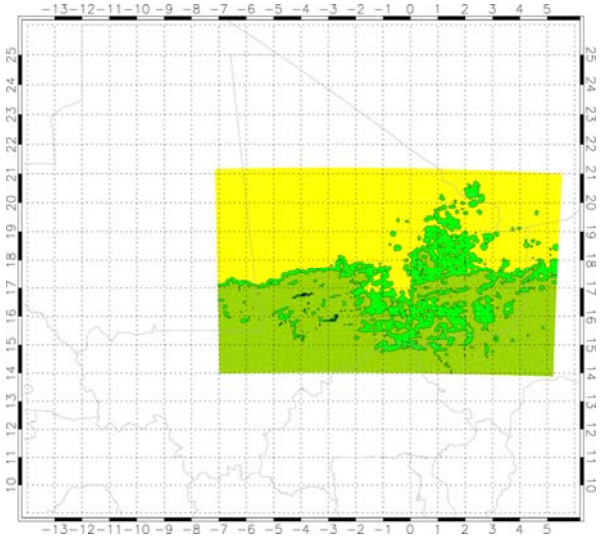

(c)

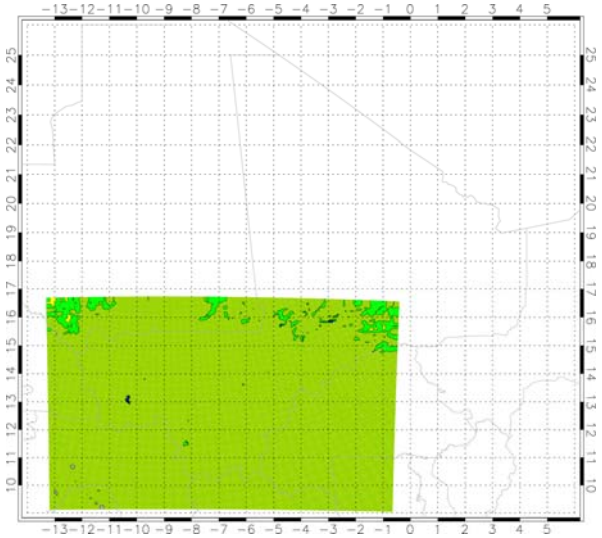

*Figure 2.2: The surface aerodynamic roughness length for the three modelling domains at a resolution of 7.5 km. The x and y axes use longitude and latitude as in figure 1.1. Colour key: Blue $z_0$ = 0.0002 m, yellow 0.0002 < $z_0$ < 0.002 m, bright green 0.002 < $z_0$ < 0.020 m, green 0.020 < $z_0$ < 0.2 m, grey 0.2 < $z_0$ < 0.60 m.. The roughness data is derived from the United States Geological Survey (USGS) Global Land Cover Classification.*

## 2.3 Initial Meteorological Data

Atmospheric data for the modelling initialization is obtained from the NCEP/NCAR reanalysis data-set on a longitude-latitude grid with a resolution of 2.5 x 2.5 degrees, Kalnay et al (1996).

Geopotential height, temperature, humidity data from the 1000 hPa, 850 hPa, 700 hPa, and 500 hPa isobaric surfaces are used. This data is converted into geostrophic wind and virtual potential temperature values for 0 m, 1500 m, 3000 m and 5500 m heights above sea level. The data is compiled into 30-year time series, covering 1977 to 2006, for use in the wind class generation programs.

## 2.4 Classification system

The time-series data of wind and temperature profiles derived from NCEP/NCAR reanalysis data is used to determine three sets of wind classes. One set for each of the modelling domains.

These wind class sets form representative sets of wind conditions for the region of interest. The wind classes represent different wind speeds, wind directions, and atmospheric stabilities.

For each wind class a wind class profile is defined. The wind class profiles describe how the geostrophic wind speed, wind direction, temperature and specific humidity vary with height, from 0 m to the top of the model at 5500 m for each wind class. The wind class profiles can be defined using all the data in the period 1977-2006 to give annual wind class profiles.

The Froude number is used to assess the likely impact of an obstacle, such as a hill, on wind flow. The Froude Number is $U / (h * N)$, where $U$ is the velocity scale, h is the height scale of obstacle, $N^2$ is the Brunt-Väisälä frequency, where $N^2 = (g/\theta_0)(d\theta/dz)$, with $(d\theta/dz)$ being the vertical gradient of potential temperature.

For cases where the Froude number is below one, the flow tends to flow around obstacles. For cases where the Froude number is above one, the flow tends to flow over obstacles. More stable conditions tend to lead to lower Froude number flow behaviour, in which channelling between or around obstacles is more prevalent, as well as lee effects to be more persistent.

The inverse Froude number squared is used in the wind class classification system to differentiate meteorological situations that have similar wind speed and direction but different thermal stratification. The height scale used is 1500 m, the height difference between the first and second level in the wind class profile.

The three wind class sets used for this numerical wind atlas study are shown in Figure 2. 3. The figures indicates the wind classes' wind speeds, directions, inverse Froude numbers squared, and frequencies of occurrence. It can be seen in Figure 2. 3 that many of the wind classes come in pairs, i.e. for similar wind speed and wind direction, two wind classes are present with different Froude number. The different Froude number reflects the wind classes' different vertical temperature profiles.

(a)

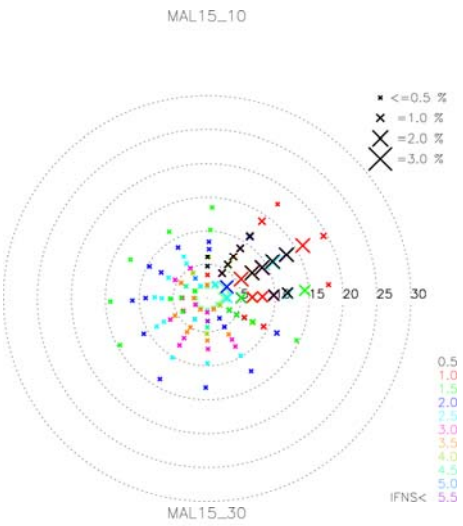


(b)

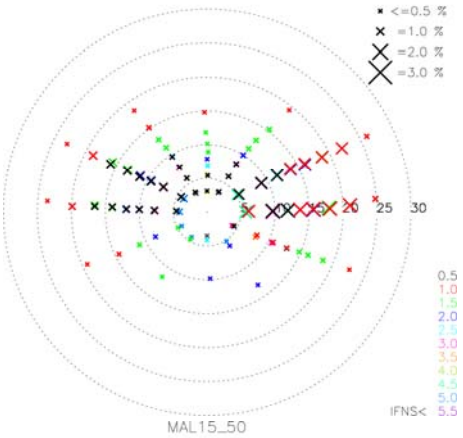


(c)

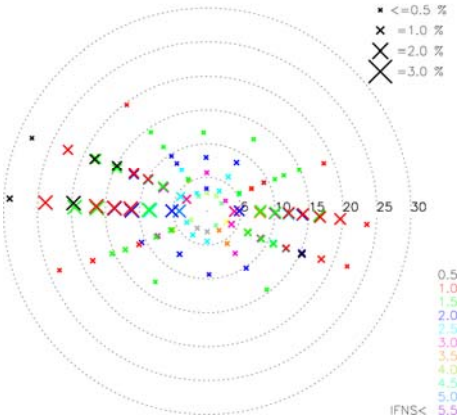


*Figure 2. 3: The three sets of geostrophic wind classes for (a) Northern Mali, (b) Central Mali, (c) Southern Mali based on data for the period 1977-2006. Each cross represents a forcing wind speed (distance from the centre of the diagram) and direction. The speed scale is in m/s. The size of each cross represents the probability of the wind class. The frequency scale is given in the upper right hand corner. The colour scale indicating the inverse Froude number squared (IFNS) is given in the lower right hand corner.*

## 2.5 Post-processing

After the mesoscale simulations are complete, the results are compiled in the post-processing stage of the methodology. First, a weighted mean of the wind speeds at each mesoscale model grid point is calculated. The weightings for each wind class simulation are based on the frequencies of occurrence. This averaging operation yields a simulated resource map. Second, for each wind class simulation, the effects of elevation and roughness variation are removed with modules similar to those in the WAsP software. Then the weighted mean of the adjusted result from the wind simulations is made. This yields a wind atlas map, or generalized wind map for flat surface condition of a specified roughness.

Figure 2.4 shows a schematic diagram of the wind class simulations and the post-processing steps.

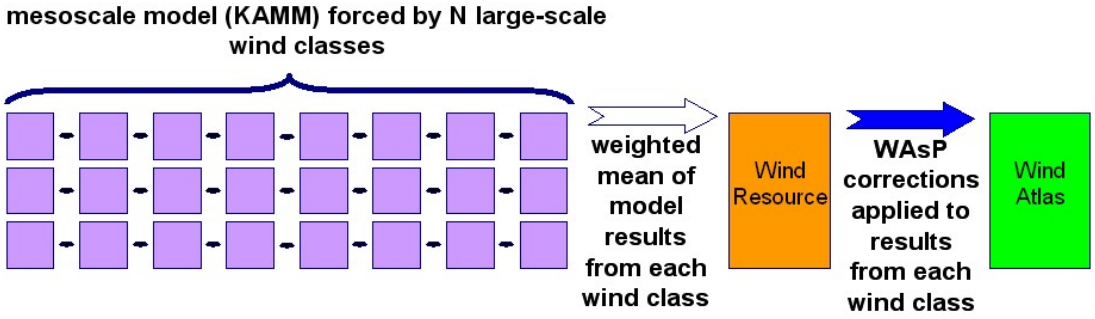


*Figure 2.4: A schematic diagram showing the KAMM/WAsP numerical wind atlas methodology. In this numerical wind atlas study, N, the number of wind classes is 136, 116, and 113, for the different calculation domains.*

## 2.6 Results

The results from the numerical wind atlas study using the KAMM/WAsP methodology can be output and utilized in two rather different ways. One way is to present the results in the form of resource maps, created in the method described above. These maps provide a good means to summarize the large amount of data generated in the study. Another way to output the results is in the form of WAsP generalized wind climate files, known as *.lib-files*, because the convention is to use the extension '.lib' in their filename.

The WAsP generalized wind climate files can be generated by the KAMM/WAsP methodology. This means that comprehensive information concerning the wind speed and direction distribution for various heights above ground level and for various surface roughness lengths can be obtained for any location within the region of interest.

WAsP generalized wind climate files will be generated on a grid with a $0.1^{o}$ spacing for the region of interest. All the *.lib-files* will be given in the database accompanying the final wind atlas provided in the next phase. A small program will also be included to assist in the selection of the appropriate *.lib-file* by prompting for the longitude and latitude of the site of interest.

Figure 2.5 shows the annual mean simulated wind respectively for the region of interest at 50 m above surface level. These maps give an overview impression of the variation of wind resources in space and seasonal.

However for any location on the map one would not expect necessarily to have measured the same mean wind speed indicated by the map. This is because the map has been created using a surface description at 7.5 km resolution. In reality the surface will be full of details in surface elevation and surface roughness. For example, small hills and forests, pertaining to elevation and surface roughness details respectively, will not be resolved.

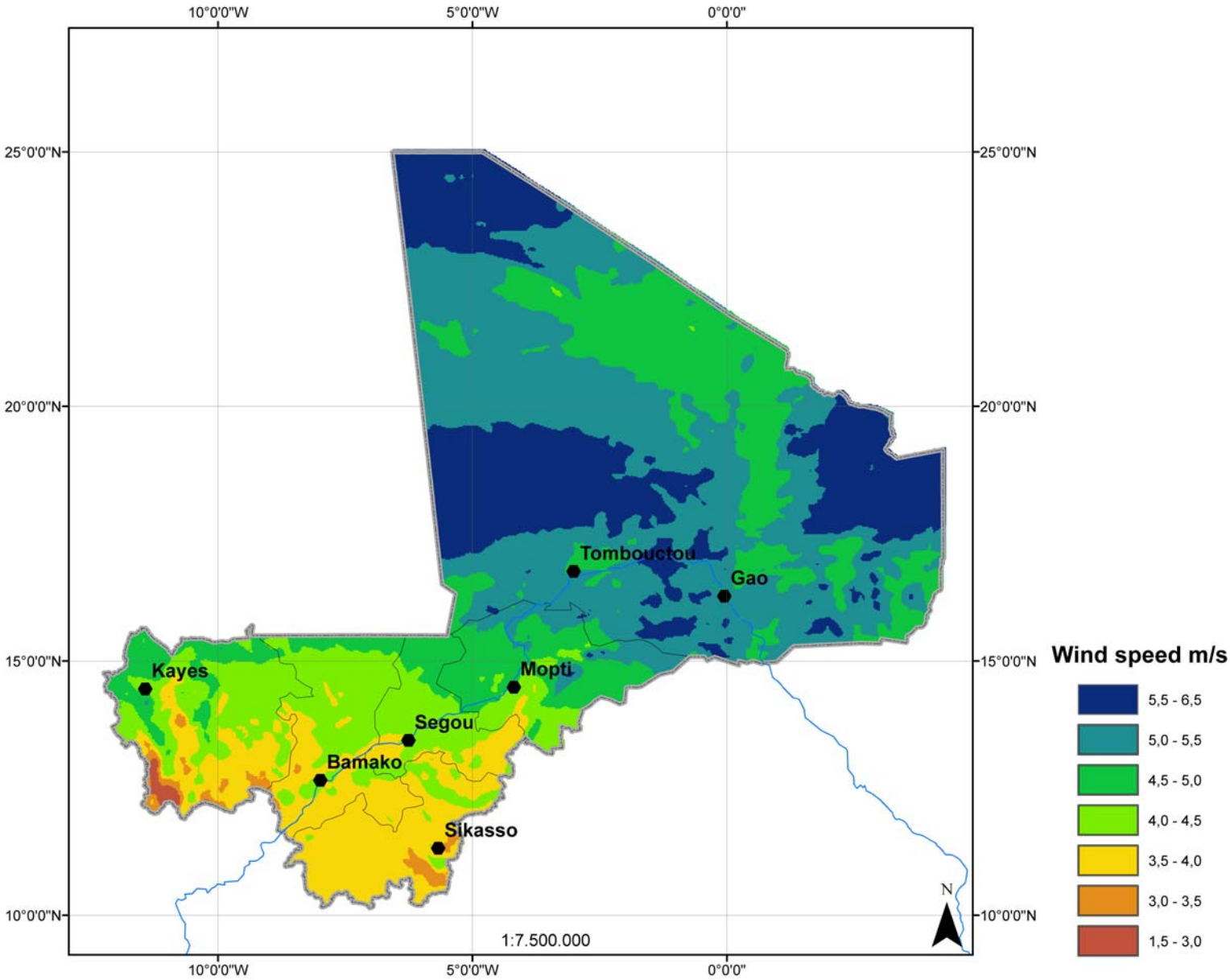


*Figure 2.5: Annual mean simulated wind speed at 50 m a.g.l. The contour interval is 0.5 m/s and colour scale is in m/s. Axes are given in longitude and latitude coordinates.*

Figure 2.6 shows the annual mean generalized wind. This map shows the resource when the effects of resolved surface elevation and roughness change are removed. It shows what the annual mean wind speed would be at 50 m above surface level for flat terrain with a uniform roughness of 0.03 m. This map is useful because it shows the mesoscale influence on wind resource, i.e. variation of resource due to phenomena other than local orographic speed-up and roughness change.

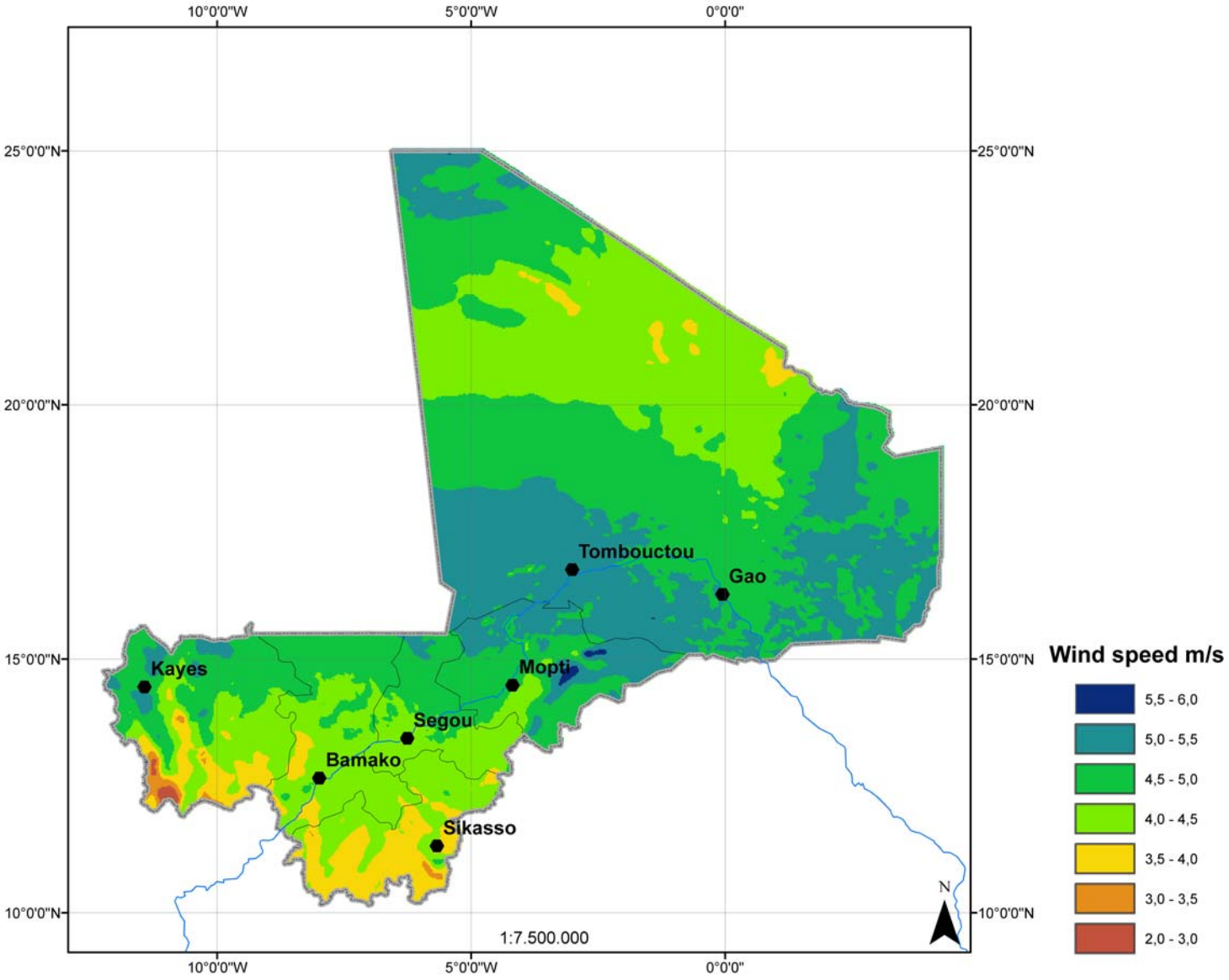


*Figure 2.6: Annual mean generalized wind speed at 50 m a.g.l. for a flat homogeneous surface with roughness length 0.03 m. The contour interval is 0.5 m/s and colour scale is in m/s. Grey contours indicating the surface elevation, country borders and coastline. Axes are given in longitude and latitude coordinates.*

Depending on local conditions, e.g. access conditions and options for replacing diesel-based electricity, wind speeds of 5 m /s are generally considered to be the

lower limit for economic feasible exploitation of wind resources. The preliminary results in figure 1.5, shows as expected a relative low (< 5 m/sec) wind resource potential in Mali, especially in the south and most populated part of the country, although exposed sites on favourably oriented ridges will give stronger mean winds. Wind speeds > 5 m/sec are prevailing in the northern part of the country, (latitude above 16 degree) including towns such as Timbuktu and Gao. Mean wind speeds of above 5 m/s are also found as far south as the Dogon plateau. Favourably exposed sites in these areas could be promising, if combined with practical utilizations possibilities. It is therefore recommended that the wind-mapping in Mali be finalized by calibrating the preliminary wind map with existing and planned ground measurements of wind-speed.

## 2.7 Error and uncertainty

The uncertainty or error on the final results of the numerical wind atlas methodology should be considered as part of the study. Each step in the methodology involves approximations and uncertainties, therefore the estimation of the final uncertainty must consider how each step may contribute to the uncertainty and characterize the impact of the error.

Contributors to the errors may include:

- Description of the large scale meteorological conditions from the NCEP/NCAR reanalysis.
    - The global NCEP/NCAR reanalysis uses a rather coarse resolution and its accuracy is better in regions of high density observations. In regions of scarcer measurement the accuracy is degraded.
    - Errors in the wind velocities may lead directly to errors in wind resource
    - Errors in temperature profiles will lead to errors in stability and Froude number, and may give rise to spurious flow behaviour in complex terrain.

- Determination of the wind class and their associated vertical profiles of geostrophic wind and temperature.
    - Breaking down a large amount of atmospheric data into approximately 120 different wind classes is a way to reduce the amount of computer resource necessary to perform the mesoscale simulations. In doing so it is possible to add new errors in the process. However great care has been taken to develop the method in which the wind classes are determined to minimize this error.
    - Certain choices for the properties of the wind classes must be made. For example, at what height should the geostrophic wind be used to define the wind classes. Careful and appropriate selection of such properties minimizes error from this step.

- Description of the surface elevation
    - The surface elevation errors may come about due to insufficient spatial resolution. One of the most serious consequences of an error in the orography is the under-representation of high terrain. For example the heights of peaks are reduced when a lower resolution is used. This may lead to incorrect interaction of flow with terrain.
    -
- Description of the surface roughness

- The surface roughness errors may come about due to insufficient spatial resolution, and also through incorrect estimation of roughness length.

- Mesoscale modelling
  - Thermally driven winds, such as sea breezes, are known to be difficult to reproduce in the mesoscale model. Since the temperatures for land and sea surfaces are held fixed in time for each wind class it is expected that evolution of such wind phenomena are not very well reproduced.
  - The KAMM modelling assumes a uniform and steady atmospheric forcing, thus any wind features due to transient and spatially varying forcings are not accounted for well.

- Microscale modelling
  - By accounting for the local mesoscale orographic speed-up and roughness change it is possible to transform the simulation wind characteristics to generalized wind characteristics (WAsP *.lib-files*). This process may introduce some uncertainties to the generalized wind statistics.

Previous numerical wind atlas studies using the KAMM/WAsP method and employing verification have demonstrated uncertainty of wind speeds at 50 m above ground level of between 5% and 15% (Mortensen et al, 2005 and Frank et al, 2001).

## 2.8 Verification

As with most modelled data generally it is of value to verify results with measurements so as to make an assessment of the error or uncertainty of the model results. The standard procedure to do this for KAMM/WAsP results is to compare generalized wind climate statistics obtained from KAMM/WAsP and from WAsP analysis of measurement data at specific measurement locations. We refer to this as 'quantitative' verification. When this is not possible then less satisfactory verification based on inspection of summary wind direction and wind speed information is required. This we refer to as 'qualitative' verification.

### 2.8.1 Quantitative

There are at least two candidate measurement locations in Mali where wind measurement have been made for the purpose of wind energy application. These measurements have been made at Gao by Deutsche Gesellschaft für Technische Zusammenarbeit (GTZ) GmbH and at Timbuktu by a Belgian agency.

In order to make the quantitative assessment it is necessary to obtain wind direction and wind speed time series data, and high resolution maps for surface elevation and surface roughness in the vicinity of the measurement station. All this is required in order to run the WAsP software in order to calculate a generalized wind climate from the observed wind climate; by accounting for local phenomena that impact measured wind speeds, i.e. speed-up due to orography and wind speed changes due to surface roughness changes.

Both GTZ and the Belgian agency have been contacted in order to obtain the wind time series data. GTZ have been able to provide part of the data, but at this time

there is still a significant gap in the data which means that no analysis is yet complete. The data for Timbuktu has not yet been obtained.

So far only a demonstration of WAsP software has been possible using the Gao site. See section 2.9. However once the data is obtained for Gao and Timbuktu then quantitative verification will be possible using WAsP.

### 2.8.2 Qualitative

To serve as a qualitative verification the generalized wind climate at Gao produced by the KAMM/WAsP numerical wind atlas methodology, shown in Figure 2.7 is compared with the summary graphs for the Gao measurement made by GTZ, shown in Figure 2.8.

Remember that this comparison is only rough because the measurement summary data includes effects due to the local topography (orography and roughness) that are not included in the KAMM/WAsP result that is why a WAsP analysis is required for a thorough verification. Also remember that the measurement data is given for 41 m a.g.l. whereas the modelled data is given for 50 m a.g.l. What is more the measurement data only applies for two years of the measurement campaign, whereas the modelled data uses large wind condition for a 30 year period.

With all these caveats in mind, it can be seen that the modelled and observed wind direction distributions are in reasonably agreement. There are two principle wind directions; north-easterly winds and south-westerly winds. Both modelling and observations indicate the north-easterly winds being more frequent than the south-westerly winds. In both modelling and observations indicate very few winds from the north-west or from the south-east.

Now looking at the wind speed distribution for all wind directions, the modelling results suggest an annual mean of 4.46 m/s at 50 m a.g.l. for flat terrain with 3 cm roughness. The observations give the annual mean of 5.3 m/s at 41 m a.g.l. but for the actual terrain and the actual roughness. The wind speed is highly sensitive to the orography, whereby a slight hill can lead to speed-up for example, and roughness. Therefore we cannot conclude that the comparison between the modelling and observed annual mean wind speed gives a disagreement. For example if the roughness at the site is lower than 3 cm, and/or the measurement mast is located on a slight hill, a WAsP analysis of the observed wind climate would lead to a generalized wind climate closer to the modelling results.

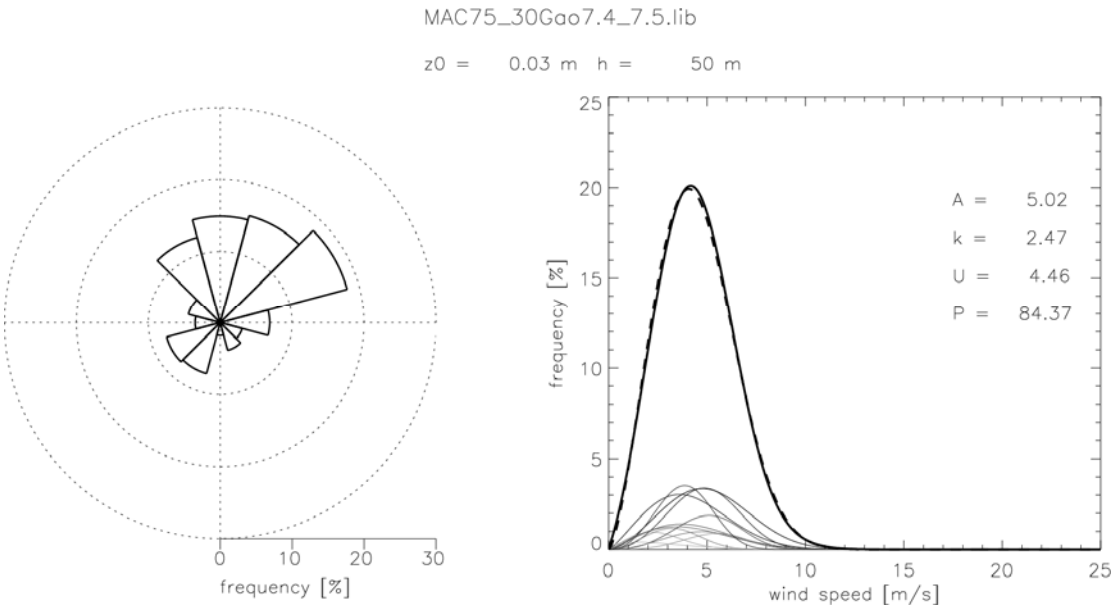


*Figure 2.7: The wind direction distribution and wind speed distribution given by the KAMM/WAsP numerical wind atlas for Gao, Mali.*

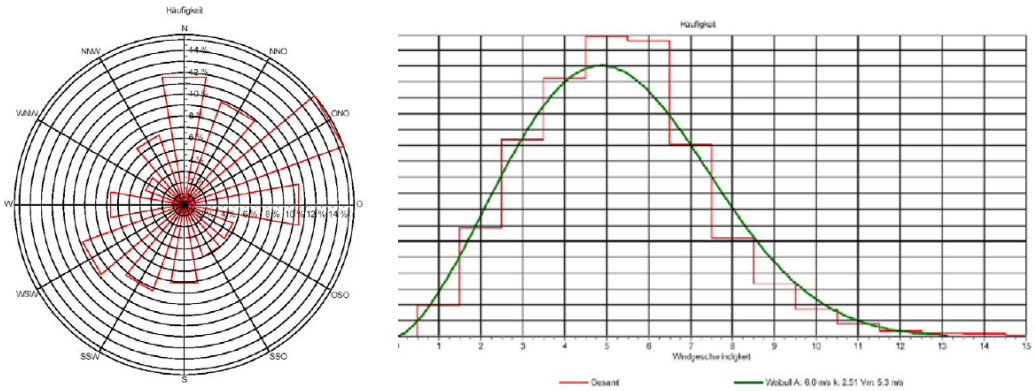


SOURCE: Aide technique aux pays du programme TERNA Mali Projet GTZ N°. : 97.2019.4-001.05 - Rapport Final de la seconde campagne de mesures
Deutsche Gesellschaft für Technische Zusammenarbeit (GTZ) GmbH

*Figure 2.8: The wind direction distribution and wind speed distribution given by measurements made by Deutsche Gesellschaft für Technische Zuzammenarbeit (GTZ) GmbH for the Gao measuring station.*

## 2.9 Application of data using WAsP

To illustrate the use of the WAsP software a demonstration calculation was set up using the orography data from the SRTM dataset and a uniform roughness of 2 cm over an area covering the vicinity of the Gao measurement station.

Figure 2.9 shows a screen shot of the WAsP software in use. The application shown has been used to calculate the variation in the annual mean wind speed over a 4.5 x 4.5 km area near the measurement station. In this example the surface roughness is 2 cm everywhere, therefore variation in wind resource is due to the orography. In a more complete example roughness change would be included and lead to further

resource variations. The software is very powerful as a tool to locate potential sites for wind turbines away from the measurement locations, and estimate the annual energy production of particular wind turbines by combining the information about directional wind speed distribution with the wind turbine power curve.

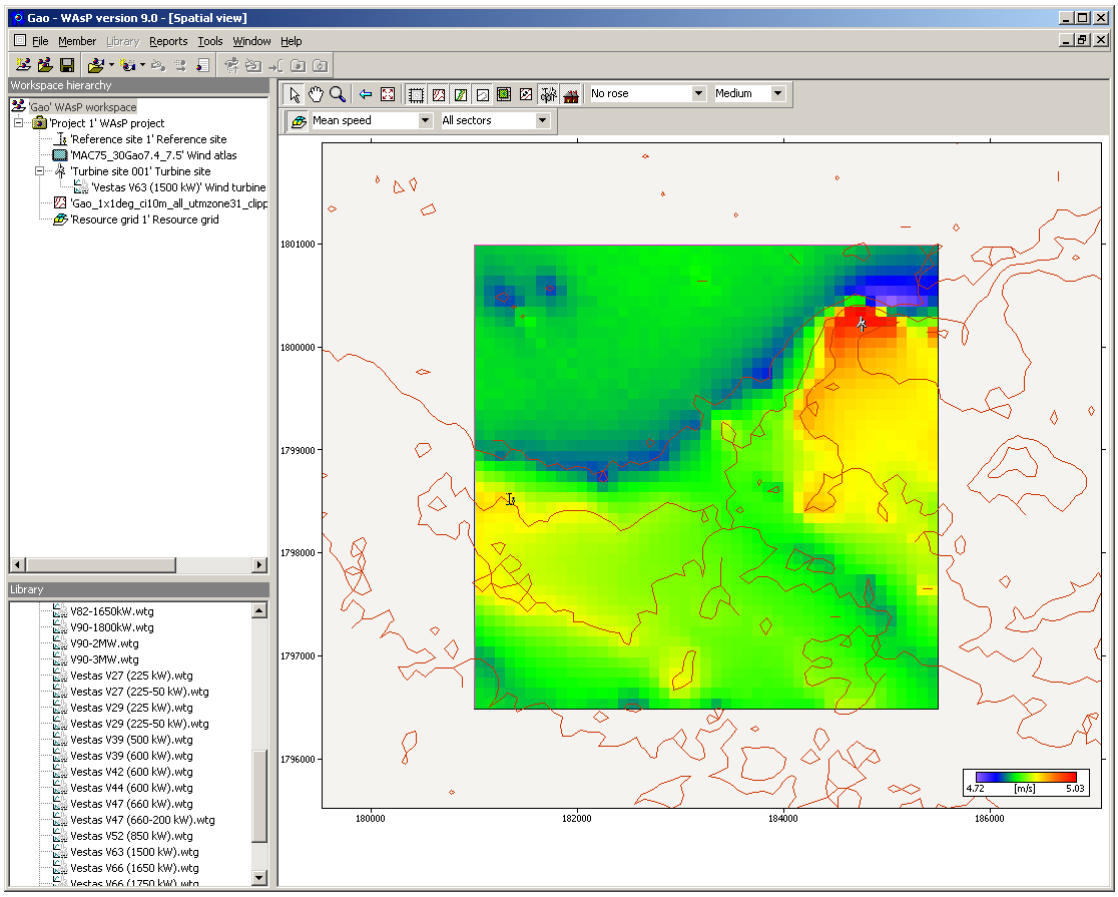


*Figure 2.9: Screen shot showing the WAsP software being used to calculate annual mean wind speed at 70 m a.g.l for a 4.5 km by 4.5 km area at 100 m resolution. The area includes the measurement station (near western edge) and a hypothetical wind turbine site (north-eastern corner). A predicted wind climate can be calculated for any location, and a estimate of the annual energy production of a wind turbine can be obtained using WAsP. The input data is generalized wind climate data from the KAMM/WAsP numerical wind atlas calculation. This calculation is an example only. Surface roughness used is 0.02 m everywhere. A site survey is needed to add more topographical detail to calculation map.*

## 2.10 Summary

The wind resource has been estimated for all of Mali at 7.5 km resolution using the KAMM/WAsP numerical wind atlas methodology. Three domains were used to cover entire country and three sets of wind classes used to capture change in large scale forcing over country. The final output includes generalized climate statistics for any location in Mali, giving wind direction and wind speed distribution. The modelled generalized climate statistics can be used directly in the WAsP software. The WAsP software then allows the inclusion of high resolution topographical information. WAsP can then used as a tool for verification studies of the KAMM/WAsP data, and for feasibility studies by calculating wind turbine annual power production estimates for any location.

First qualitative comparison with wind measurements (Gao) indicates broad agreement of KAMM/WAsP and observations However to make quantitative verification numerical wind atlas study the measurement time series data, and high resolution information for the topography around measurement station is required. Gao and Timbuktu present two candidates for verification locations and steps are underway to obtain the time series data. Even a limited verification of the numerical wind atlas data using any available measurement time series data, of good quality, and is valuable for assessing the uncertainty of the modelled data.

The preliminary results show a wind resource, which is relatively low, but which under certain conditions will be economically feasible, i.e. at favourably exposed sites, giving enhanced winds, and where practical utilization is possible, given consideration to grid connection or replacement or augmentation of diesel-based electricity systems. It is therefore recommended that the wind-mapping in Mali be finalized, by calibrating the preliminary wind map with existing and planned ground measurements of wind-speed.

## 2.11 Acknowledgments

NCEP/NCAR reanalysis data are provided by the National (USA) Center for Environmental Prediction (NCEP) and the National (USA) Center for Atmospheric Research (NCAR). SRTM data is provided by the National (USA) Geospatial-Intelligence Agency (NGA) and the National (USA) Aeronautics and Space Administration (NASA). The roughness data is derived from the United States Geological Survey (USGS) Global Land Cover Classification. KAMM is used with kind permission from Karlsruhe University, Germany.

Deutsche Gesellschaft für Technische Zusammenarbeit (GTZ) GmbH: are thanked for providing measurement data for Gao from the project “Aide technique aux pays du programme TERNA Mali Projet” GTZ N°. : 97.2019.4-001.05 “Rapport Final de la seconde campagne de mesures”.

# 3 Solar energy resource assessment

## 3.1 Methodology[1]

The estimation of global radiation by satellites is generally based on estimation of the cloud cover, since the cloud cover is the main factor determining the reduction of the incoming solar radiation (Möser & Raschke, 1983). Images acquired by METEOSAT-8 (also known as Meteosat Second Generation – MSG) are especially useful for this as the satellite performs a scan of the earth disk every 15 minutes making it possible to monitor the temporal distribution of clouds and thereby solar radiation with a 15 minute temporal resolution. The spatial resolution of the visible channels required for this monitoring is 3 – 5 km over West Africa. For Mali a consistent spatial resolution of 4 x 4 kilometres has been chosen.

The methods for determining global radiation by means of geostationary satellites are many. They are generally divided into two groups, the physically based and the statistical methods. The physically based methods combine radiative transfer calculations with satellite derived parameters (Möser & Raschke, 1983), whereas the statistical methods use empirical relations between radiation measurements at the ground and radiation estimates from satellite images (Cano et al., 1986). The first successful attempts are described in (Tarpley (1979) and Gautier et al. (1980) and later by Möser & Raschke (1983) and Cano et al. (1986). Applications of the method developed by Möser and Raschke (1983) are described in Möser & Raschke (1984) and Tuzet et al. (1984) and improvements to the method in Stuhlmann et al. (1990). The statistical method of Cano et al. (1986) has been developed further in the Heliosat project, (Diabaté et al., 1988) and (Beyer et al., 1996). Beyer et.al (1996) has presented a simple routine, and the approach selected for the present study is very similar although some modifications to the clear sky radiation model has been introduced based on the work by Ineichen & Perez (2002).

### 3.1.1 Global radiation estimation from satellites

Through image processing a cloud index n, is determined using data from the visible channel of the METEOSAT-8 sensor. The simple and widely used expression for the cloud index n introduced by Möser & Raschke (1983) is defined as follows:

$$n = \frac{\rho - \rho_{gr}}{\rho_{cl} - _{gr}} \qquad (1)$$

where $\rho$ is the pixel reflectance for a given image pixel, $\rho_{gr}$ is the reflectance of the ground under clear skies and $\rho_{cl}$ is the reflectance of a thick compact cloud cover.

The ground reflectance is mainly affected by changes in solar altitude, vegetation cover and soil conditions (Stewart et al., 1999). Since the conditions that effect $\rho_{gr}$

1 The adapted methodology for assessing the spatial and temporal distribution of solar energy in Mali builds on the methodology developed by Simon Stisen in his PhD thesis from 2007 from the Institute of Geography and Geology, University of Copenhagen, Denmark entitled "Distributed Hydrological Modelling and R.S". Simon Stisens work focused on the Senegal Basin so a number of adjustments have been made in order to process the data covering Mali with the most important being the adaptation to MSG instead of Meteosat-7 and the inclusion of the Linke turbidity factor representative for Mali. The methodology paragraph here is based on the methodology description from Simon Stisens thesis

changes in both time and space $\rho_{gr}$ needs to be determined as a series of maps of minimum reflectance. In principle one minimum reflectance map is required for each acquisition time during the daylight period. But since clouds will contaminate the minimum reflectance maps, these have to be constructed as minimum composites of a series of images from the same time of the day. The number of images that are used for each map is a compromise; long enough for all pixels to be cloud free and short enough for changes in surface reflectance to be small. In this setup the period was set to one month due to frequent clouds at various parts of the area at varying times.

The maximum reflectance $\rho_{cl}$, is calculated as a function of the solar zenith angle (SZA). The relation between $\rho_{cl}$ and SZA is derived from an evaluation of the $\rho_{max}$ − SZA space for all daytime images. The method includes the assumption that the incoming global radiation at the ground $R_s$ is a function of the clear sky or extraterrestrial global radiation $R_{s0}$ and a function $k(n)$ depending linearly on the cloud cover index (Beyer et al., 1996).

$$R_s = k(n) \cdot R_{sO} \tag{2}$$

$$k = a \cdot n + b \tag{3}$$

The assumption that incoming global radiation $R_s$ only depends on the clear sky radiation and the cloud cover, neglects the effects caused by diffuse radiation.

To determine the regression parameters $a$ and $b$ empirically, a set of hourly recorded ground measurements of global radiation and satellite derived n-values for the same time and place, are ideally required to take regional factors into account. However, due to both the size of the area and lack of suitable in-situ data the model has been run with the standard parameters for $a$ and $b$ as suggested in the original work by Ineichen & Perez (2002). The clear sky radiation $R_{s0}$ is dependent on a range of factors including the solar constant $I_0$, the sun-earth distance $e$, the solar altitude angel $\gamma_s$, optical air-mass $am$, altitude and the turbidity and water content of the atmosphere (Iqbal, 1983). The clear sky model described in Ineichen & Perez (2002) was chosen for this study since it implicitly takes into account air-mass, Linke turbidity TL and altitude. Data on the Linke turbidity factor was obtained from the SoDa database (SoDa, 2007).

Under the assumption that the k-n-relation applies for the entire area under investigation the clearness index $k$ can be estimated. All equations are summarized in equation (4):
m

$$R_{s,d} = \sum_{p=1}^{m} (R_{s0}(a \cdot n + b) \cdot dt \tag{4}$$

where $R_{s,d}$ is the daily sum of global radiation [Wh m-2], $R_{s0}$ is the clear sky global radiation [W m-2], $n$ is the satellite derived cloud cover index [-], $m$ is the number of daily satellite images [-], $dt$ is the time interval between satellite images [h] and $a$ and $b$ are empirical constants.

A graphical illustration of the work flow is given below in figure 2.1 with illustrations taken from Senegal:

Reflectance, $\rho$

Cloudfree reflectance, $\rho_{cloudfree}$

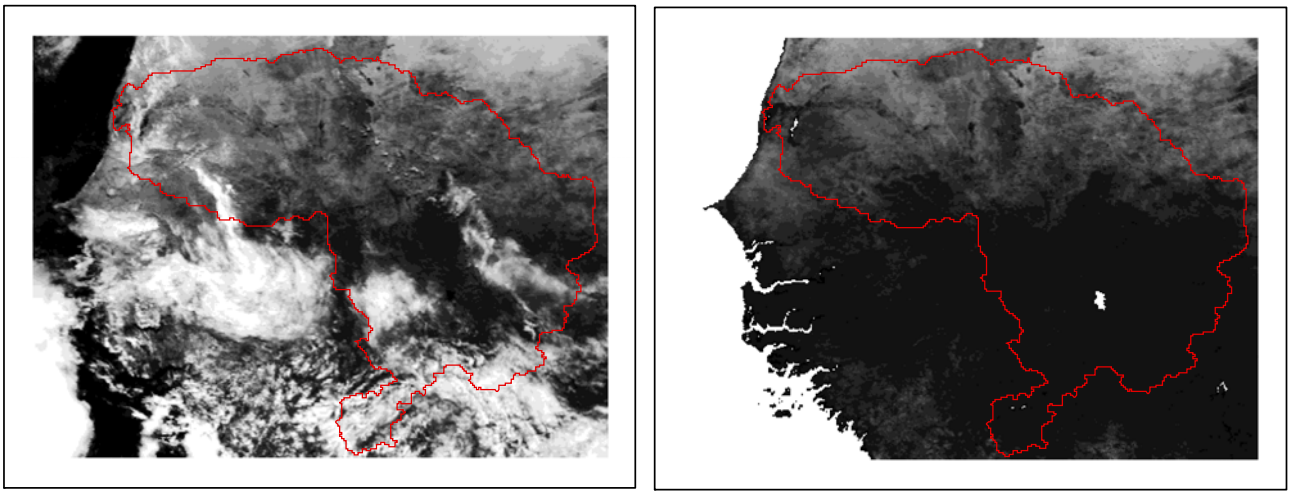

Instantaneous $R_s$:

Cloud cover index, n

Incoming solar radiation, $R_s$

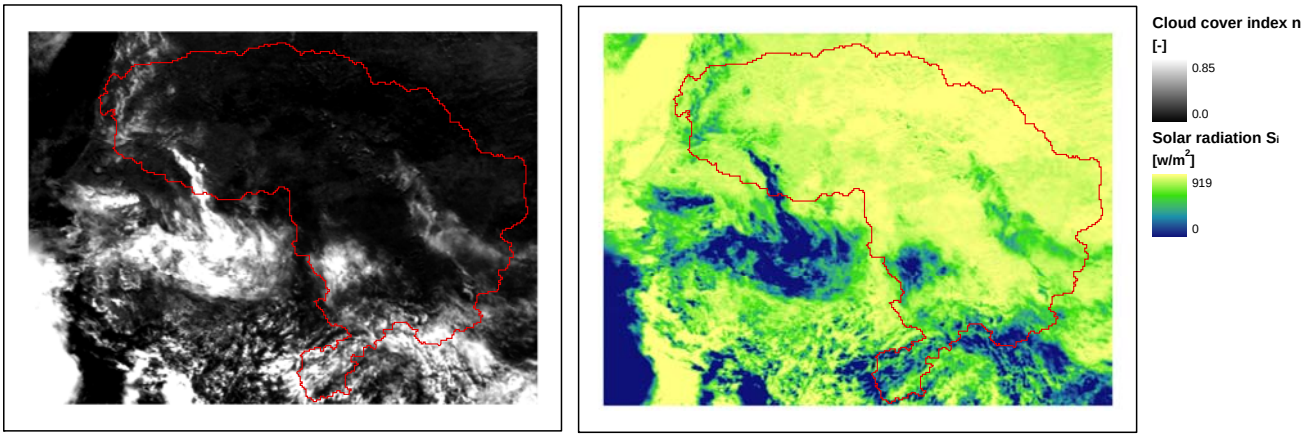


*Figure 2.1: Steps in the estimation of solar radiation*

### 3.1.2 Computation – practical issues

*Linke Turbidity*

As mentioned the Linke turbidity factor has been found from the SoDa webpage: http://www.soda-is.com. Output from the service are monthly values. A single monthly value has been applied for the entire area; data was extracted for central part of Mali:

| Tam: Linke turbidity factor, monthly mean, climatological values, unit= [ ] | |
|---|---|
| **Month** | **TL** |
| Jan | 5.6 |
| Feb | 5.7 |
| Mar | 5.8 |
| Apr | 6.2 |
| May | 6.1 |
| Jun | 6.5 |
| Jul | 6.5 |
| Aug | 6.8 |
| Sep | 6.6 |
| Oct | 6.0 |
| Nov | 5.7 |
| Dec | 3.9 |

*Missing data*

From the more than 12000 satellite images needed to cover the calendar year of 2006 some gaps in available data was encountered. The periods with missing data has been filled by created a simple average of the reflectance map immediately before and after the time of missing observation. If case of two or more missing observations found in conjunction a simple average was made based on the observations from the same time of day for the day before and after the missing data. There was a longer period of missing data in the period September 23$^{rd}$ – October 5$^{th}$. This gap of 13 days was filled by creating a simple average of the 5 days immediately before and after the period. By basing the average of a total of 10 daily images a representative level of cloud cover variance has been included and by taking data from before and after the period the effect of change in incoming radiation due to changing sun illumination and position has been minimized:

.

| Month | Number of potential acquisitions | Number of missing acquisitions |
|---|---|---|
| Jan | 1023 | 14 |
| Feb | 924 | 2 |
| Mar | 1023 | 3 |
| Apr | 990 | |
| May | 1023 | 12 |
| Jun | 990 | |
| Jul | 1023 | |
| Aug | 1023 | |
| Sep | 990 | 245 |
| Oct | 1023 | 139 |
| Nov | 990 | |
| Dec | 1023 | |

## 3.2 Results

The output of the work flow is maps covering Mali showing the actual spatial distribution of solar radiation at a specific time with a 15 minute interval during 9.00 – 17.00 every day. These maps have been summarized to produce daily, monthly and a yearly map. For details of the monthly distribution and variation please consult appendix A.

The yearly sum of all solar radiation is shown in the figure 2.2 below. The values ranges from 1650 – 2000 kWh/m$^2$ with the general trend of larger values in the South - South eastern part of Mali and the smaller values in the North - North eastern part.

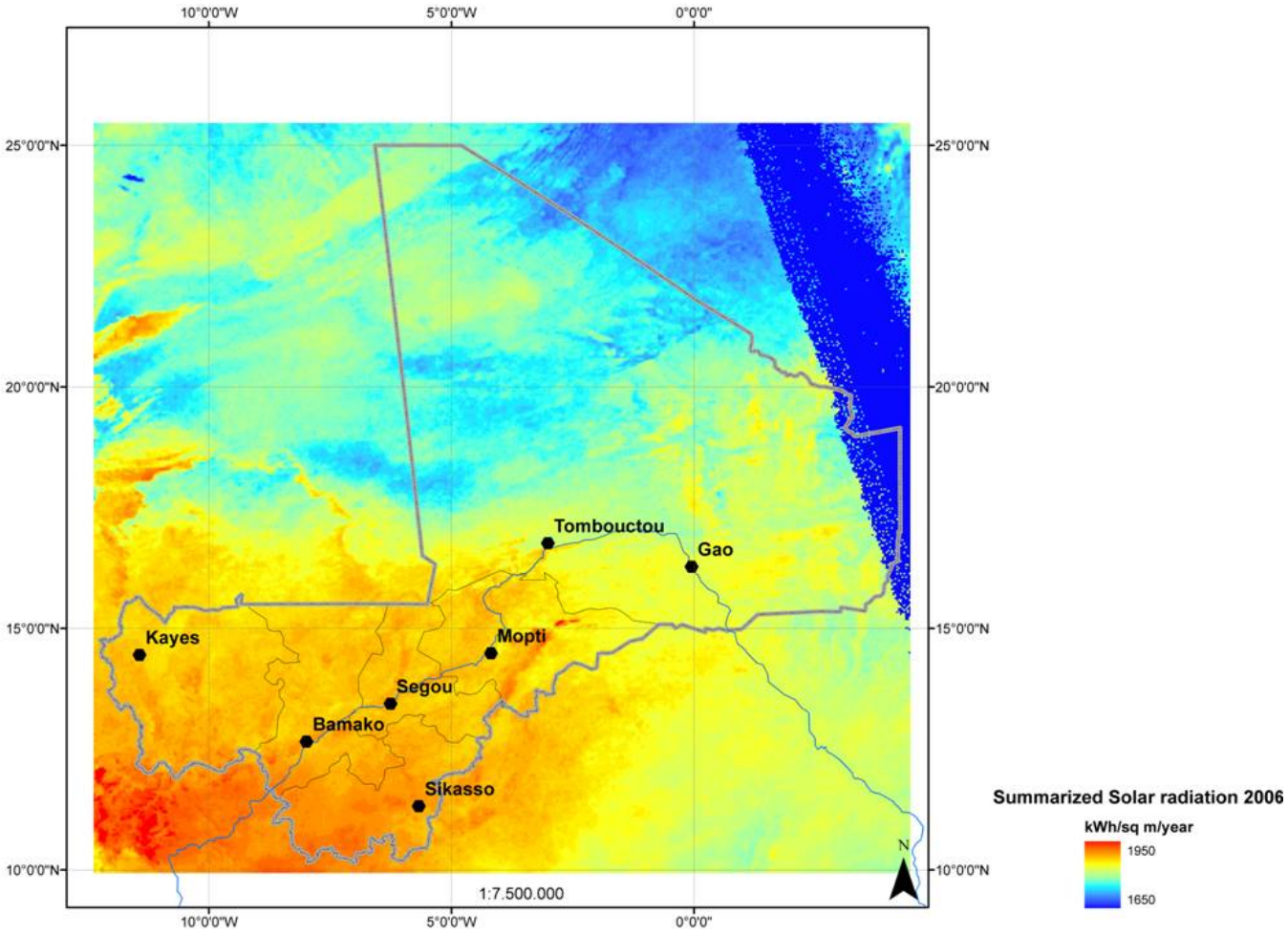


Figure 2.2: The total solar radiation input for 2006

## 3.3 Validation

In order to validate the extracted solar radiation results it is necessary to have access to measured reference data. During a trip to Mali in November 2007 it was examined if any in-situ data were available. With good assistance from local experts and especially from Professor Diabate, School of Engineering, it became clear that no available measurements are available in Mali.

An attempt was made to compare the results with data from the NASA dataset Surface meteorology and Solar Energy (SSE) (POWER/SSE Release 6.0). This dataset has recently been updated so it now has global coverage of daily data on insolation incident on a horizontal surface (kWh/m2/day) for the period 1983 – 2005. The data is available in tabular form on a daily basis or as monthly means for a specific area. The spatial resolution of the data is very coarse (1x1 degree) and the data is based on integration of a number of different data sources including various satellite observations and ground based measurements of several parameters.

The comparison was performed on 3 different sites in Mali – North, Central and Southern part; see figure 2.3 for location – where daily data was extracted for a single 4x4 km pixel.

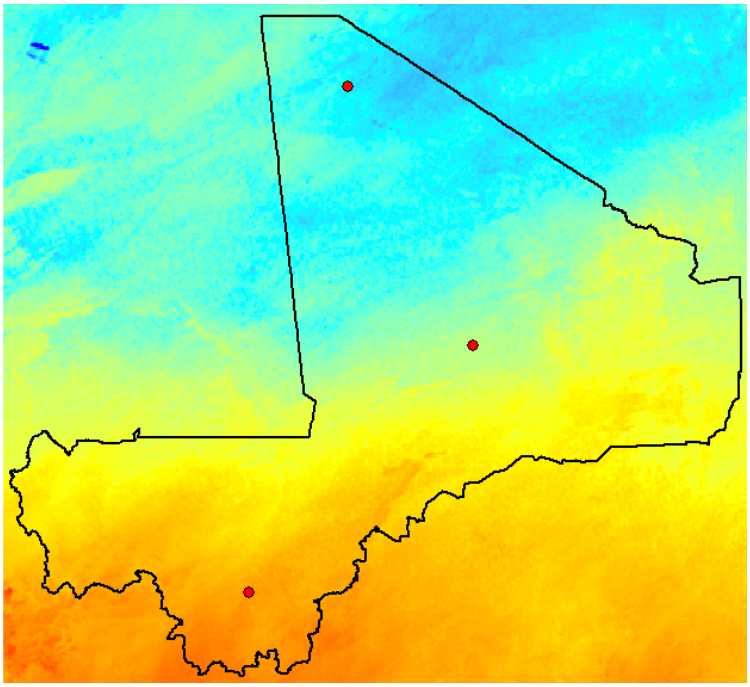

*Figure.2.3: Location of the three areas where data has been extracted from the MSG radiation data for the year 2006.*

The data from the 3 different places reveal the inter-annual variation going from North to South which is a function of both the position of the sun and the cloud cover. In the north a more traditional 'bell shape' curve is found with values ranging from app. 4000 to 7000 $Wh/m^2$/day over the year. Going southwards the annual variation in solar radiation becomes less pronounced reaching a constant level of 5000 – 6000 $Wh/m^2$/day in the southern part of Mali. The daily data plot (figure 2.4) show the daily variation is bigger in the southern region of Mali due to varying cloud cover especially in the period from May – September. The inter-annual variations are more clearly shown in the monthly average plot shown in Figure 2.7 – 2.9.

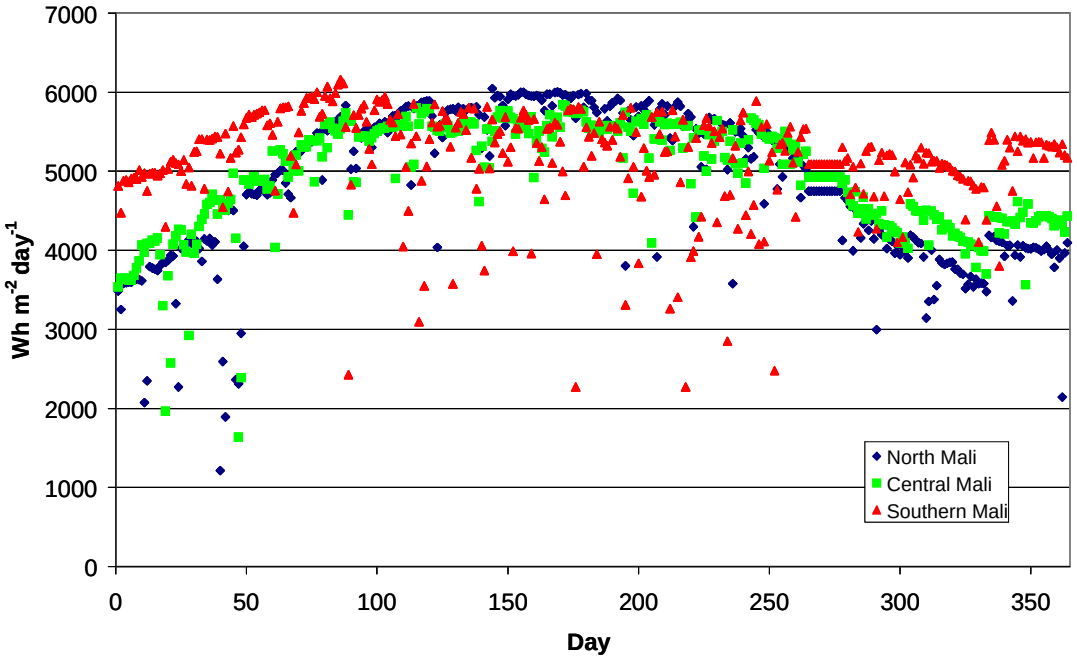


*Figure 2.4: Daily radiation data from the three locations where data has been extracted from the MSG based radiation data from 2006.*

The comparison between the NASA Solar data and the MSG based data showed a consistent underestimation of the MSG based monthly average values. Given the fact that the current methodology is based on global coefficients and no local adjustments have been made the result is considered very promising. The spatial and temporal variation in the solar radiation is clear from the MSG data even if the actual values are underestimated in absolute terms. If good quality in-situ measurements had been available a local calibration of the model would have been feasible and the MSG data could have been adjusted to the higher level suggested by the NASA data. A significant improvement would be to include a locally adjusted expression for additional diffuse radiation and less important a description of the effect of the chosen day length. With an MSG observation window from 09.00 – 17.00 a small part of the radiation is omitted in the dawn and dusk periods. The work by Simon Stisen (Stisen, 2007) showed that with a local calibration of the MSG method a RMSE 5 – 17 W/m$^2$ was found – corresponding to app. 6 % of the average daily global radiation (Figure 2.5):

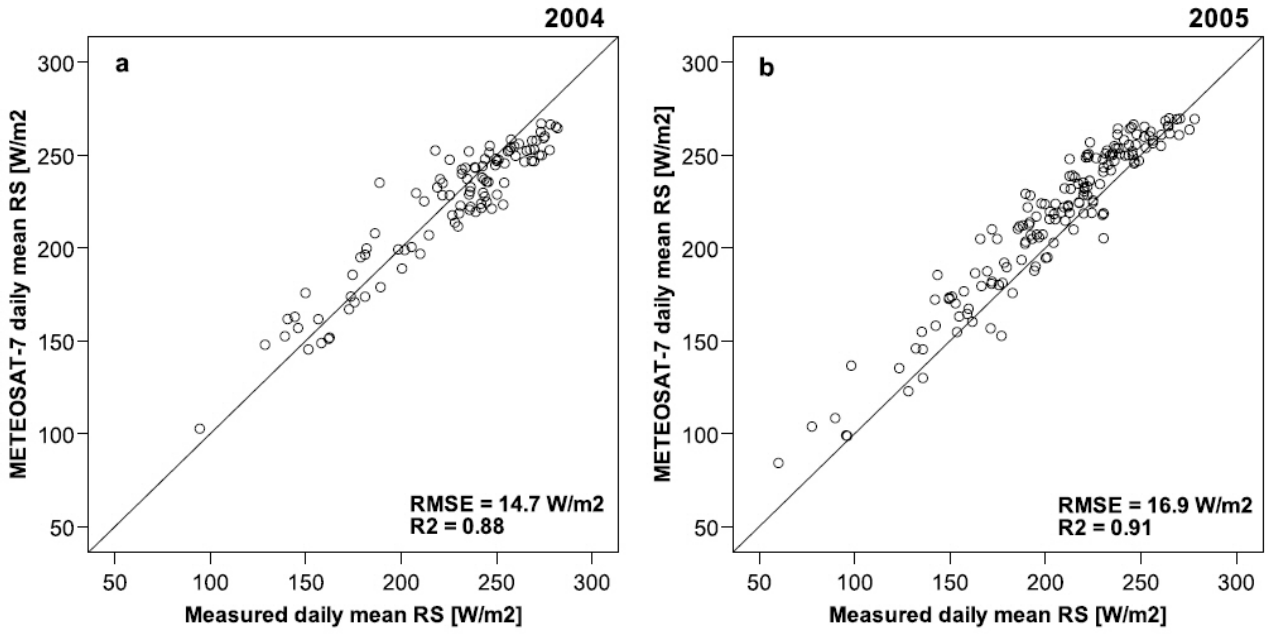


*Figure 2.5: Result of locally calibrated MSG based radiation retrieval from Senegal (Stisen, 2007)*

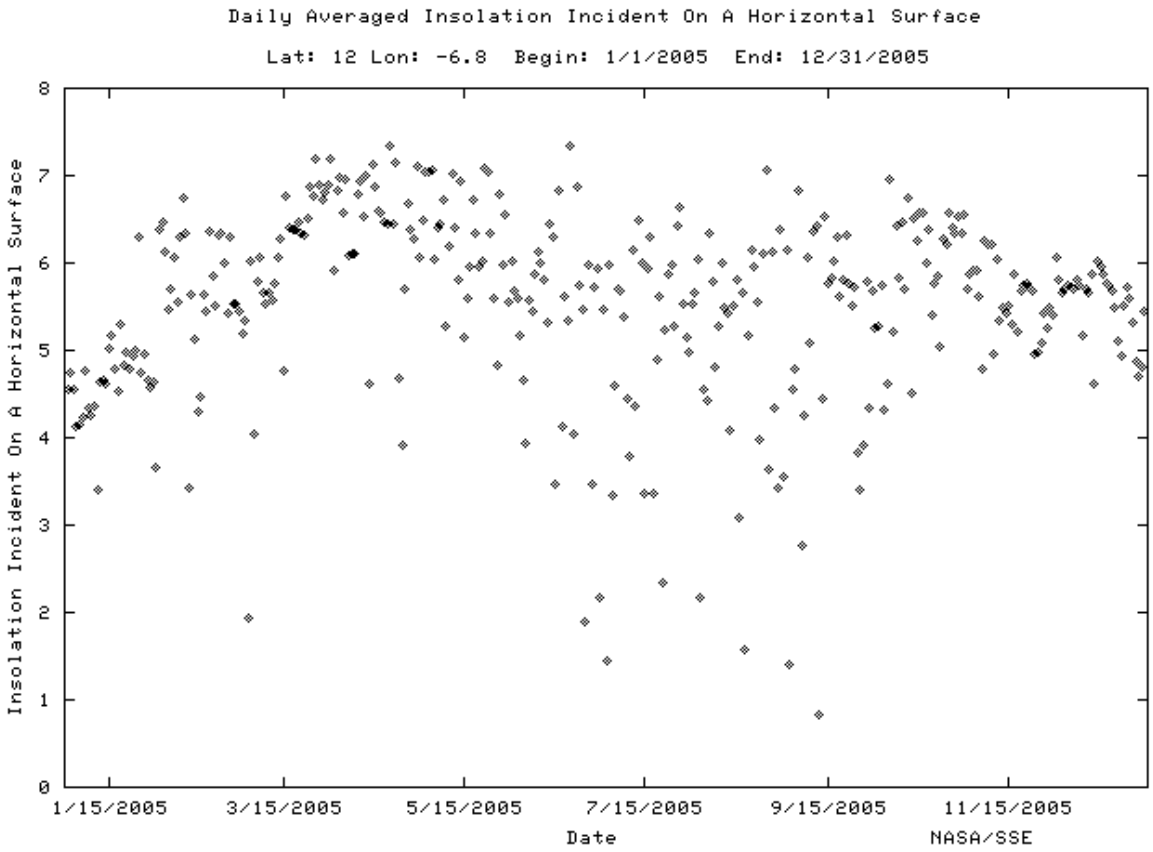


*Figure 2.6: Extract from the NASA PPOWER/SSE data set. The data shown is daily data from 2005 for the 1x1 degree tile where the southern area is located.*

When comparing the result with the NASA data it is also important to take the nature of the NASA data into account and acknowledge the shortcomings of that data set – the major ones being that the data is available in 1x1 degrees cells only and that it is a mix of several data sources with varying temporal and spatial resolutions. Also, the data presented here are average monthly values for the entire period 1983 – 2005. The day-to-day variation found in the NASA data is more pronounced than in the MSG based radiation data as shown above in figure 2.6.

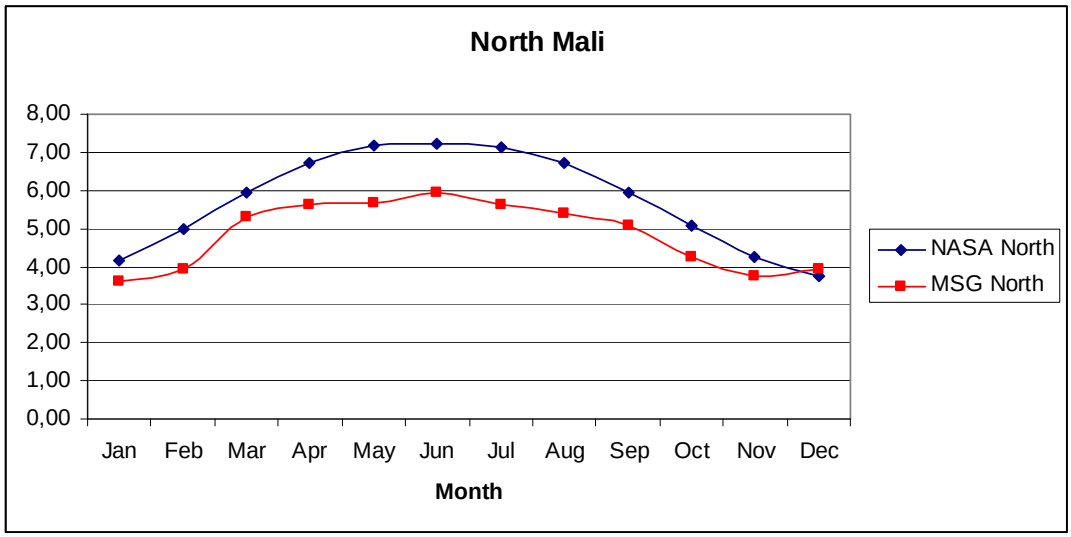


*Figure 2.7: Comparison between MSG derived radiation and NASA solar radiation data for the northern part of Mali. Units are kWh/m2/day.*

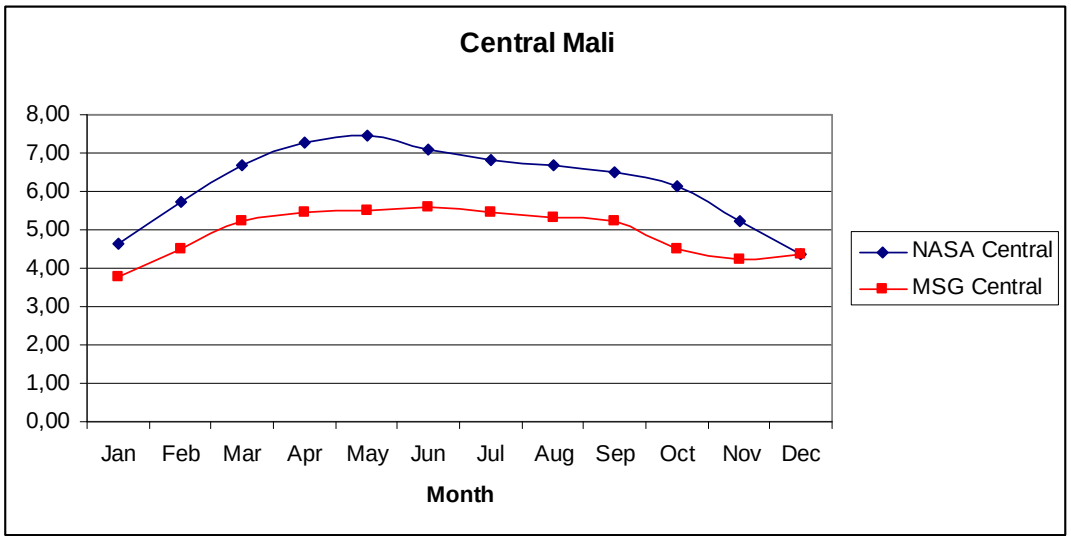


*Figure 2.8: Comparison between MSG derived radiation and NASA solar radiation data for the central part of Mali. Units are kWh/m2/day.*

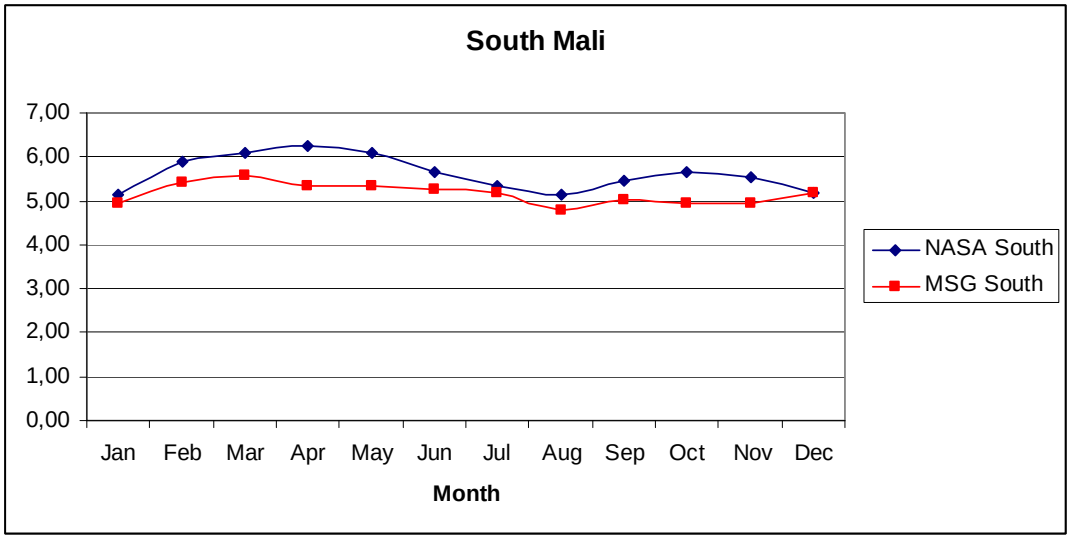


*Figure 2.9: Comparison between MSG derived radiation and NASA solar radiation data for the southern part of Mali. Units are kWh/m2/day.*

## 3.4 Discussion and conclusions

The results reported contain far more information on spatial and temporal variability of the solar power potential than alternative data. Differences in absolute values between the current estimation and other data-sets are present, and need to be resolved by more ground measurements.

The accumulated annual solar radiation input varies less than 20 % within Mali, with the highest values in the South, as shown in figure 2.2. The monthly accumulated values, illustrated in map form in appendix A, show considerably greater variation. It is interesting to note that the radiation inputs in the North and South of Mali are out of phase, highest in the South in the months of October-April, highest in the North in the period of May - September.

# 4 Biomass resources assessment

## 4.1 Introduction and objectives

Biomass, mostly in the form of fuel wood, is the most important component of the traditional energy system of Mali, and in particular in the rural areas. The present analysis does not intend to assess the importance of biomass resources used in this traditional way. Rather the objective is to assess the potential for certain alternative uses of biomass in a future energy system of Mali. These alternative uses include:

- Use of presently unused dry biomass resources, such as agricultural residues, for fuelling power generation in power plants
- Use of presently unused biomass resources, such as agricultural residues, for producing bio-ethanol, using 1st and 2nd Generation technologies
- Production of crops, such as cassava, specifically for bio-ethanol production
- Production of crops, such as *Jatropha carcus,* for bio-diesel purposes

It is beyond the scope of this pilot-study to make an accurate assessment of these four options. In order to provide a rough estimate of the overall potential, we have focused on estimating the basic resource, the 'net primary productivity' (NPP). The estimate is based on deriving a proxy for NPP from time-series of satellite images.

It should be noted (and will be discussed below) that there are two basic limitations to using current NPP as a measure of the basic resource: Firstly, a high demand for biomass for energy purposes will lead to an increase in prices, which may cause farmers to use greater amounts of inputs, which in turn may increase NPP. Thus the basic biomass resource, on which all the above contributions to the energy system are based, is not fixed. Secondly, it is very difficult to estimate how much of the NPP is actually available for energy purposes: Biomass may be harvested for human consumption, it may be grazed by livestock, it may be burned in controlled or uncontrolled fires, and it may decay after the end of the growing season. Field work has been conducted and secondary data collected to give a preliminary assessment of the fraction of NPP available for energy purposes. The results of the estimation of NPP should be interpreted with these limitations in mind. Yet we have used the NPP estimates, along with information on land use and agricultural systems, to point to areas that may have a potential for producing biomass for energy purposes.

As indicated, biomass, both in natural vegetation and in crop residues, may be used either for combustion in a power plant or for production of liquid bio-fuels. In some cases these two uses of biomass may compete for the same biomass resources. Maize may be a current example of this, and in the future, when 2nd Generation ethanol production technologies become available, straw from grain production in general, residues from cotton production and woody material may be used for both purposes. We have not entered into an assessment of which of the two uses of biomass is likely to be the most realistic and favourable.

There are several partial studies of agricultural residues in Mali available for energy purposes. A review of these studies and a review of existing projects utilizing biomass for energy purposes have been carried out as part of this preliminary study. This review is presented as appendix B.

## 4.2 The sustainability of producing bio-fuels

The cultivation of crops specifically for production of bio-ethanol or bio-diesel is an issue of intense debate. The current steep increases in prices of food crops are to some extent attributed to the increasing demand for bio-fuels, mainly caused by the US and European goals of replacing 5 – 10% of the gasoline/diesel by liquid bio-fuels. The effects on living conditions and food security of vulnerable population groups in the LDCs are in focus. Also the environmental sustainability of bio-fuel production is debated, both because the seemingly $CO_2$-neutral bio-fuels may actually be produced at the expense of relatively large emissions of greenhouse gases, and because other scarce resources (of water and soil nutrients) may be depleted by the production of feedstock for bio-fuel purposes. On the other hand, certain feedstock production systems may not suffer from these problems, and the increase in agricultural prices, caused by the demand for bio-fuels, may be to the advantage of countries, such as Mali, depending to a great extent on the agricultural sector. While this is a discussion of great strategic importance to Mali, it is not the objective of the pilot project, reported here, to enter into such analyses. It suffices to note that if production of feedstock for liquid bio-fuels is to develop, certain production systems may be less problematic than others. A few currently known examples may be:

- Production of plant oil for bio-diesel from the fruits of *Jatropha carcus*, as already widely promoted in Mali
- Production of cassava as a feedstock for bio-ethanol (existing 1st Generation technology) in areas with low intensity land use
- Use of straw from grain production (e.g. rice in the inland delta of Niger), residues from cotton production and woody residues from forestry as feedstock for bio-ethanol (presuming that 2nd Generation technologies become available).

## 4.3 Sensitivity of biomass production to climate change

Mali is located on a steep climatic gradient from the vast hyper-arid expanses in the North to areas with more than 1000 mm of average annual rainfall in the Fouta Djalon in the South. Therefore it is exposed to the effects of variations in intensity and N-S location of the ITCZ, causing great inter-annual variations in rainfall. The great drought of the 1970's and early 80's is a good example. This drought is one of the most significant climatic anomalies of the 20th Century, even seen in a global perspective. The NPP and biomass resources of Mali are, of course, strongly affected by such anomalies and trends, and given the long investment horizons involved in building up a national energy system it is worthwhile to consider whether development plans are 'climate proof'. Analyses of satellite data have shown that there is a strong spatial and temporal correlation between annual rainfall and NPP, as long as the annual rainfall is less than about 700 mm. In higher rainfall areas the dominating limiting factor for NPP is soil nutrient availability, along with several other factors. Since most of Mali receives less than 700 mm annual rainfall, this implies that an energy system based mainly on biomass (natural vegetation as well as rainfed crops) will be very sensitive to climate change. There is currently no clear indication of the size – and even direction – of the changes in precipitation which may be expected to take place due to the increased concentration of greenhouse gases in the atmosphere, as clearly illustrated in IPCC's 4th Assessment Report (Christensen, 2007). The 30 models used to predict climate change globally strongly disagree on whether an increase or a decrease should be expected. The disagreement on the sign of the trend does not reflect that most models predict little change: Actually, some predict quite substantial changes, yet in opposite directions. Thus,

basing an energy system mainly on biomass appears to increase the vulnerability of the energy system to climate change.

## 4.4 Methodology

We will apply a two-step approach to the assessment of biomass resources /NPP. At the national scale we will use data on NPP and land cover to provide an overall picture of the spatial distribution of NPP. We will use this information as a basis for selecting a number of sites for which field work on the use of biomass is subsequently to be carried out, and for which secondary information is to be collected. The main idea is to give an overall picture of where NNP is high enough, at the regional scale, to support its use for energy purposes, and where the alternative uses and losses of biomass, for food, fodder and as fuel for burning, could be limited.

Subsequently, four areas have been selected for a more detailed analysis. In the pilot project, reported here, only a very preliminary analysis of these selected sites will be made. The areas have been selected with a view of their expected potential as suppliers of biomass for energy purposes. They include the inland delta with large-scale irrigated rice production and thus substantial amounts of agricultural residues. Two areas around Sikasso and Koutiala have been selected, since they represent areas with relatively high NPP in intensively cultivated regions with a potential for using agricultural residues. Finally, an area in the woodland zone to the south has been included, because of its high NPP as well as a high yield potential for crops (incl. cassava) for bio-fuel production.

### 4.4.1 Estimation of NPP by use of satellite images.

Strictly speaking, NPP is the total photosynthetic gain of plant material (measured as dry weight or as the weight of carbon) per unit ground area minus respiratory losses. For a given period, this is equal to the change in plant biomass (assuming negligible losses due to grazing) measured for both above ground and below ground plant parts.

NPP has traditionally been measured on plot size areas of land and subsequently extrapolated to larger areas. This has proven suboptimal due to large variations in biomass production even over small distances. The number of small plots of land to be measured in order to produce national estimates of biomass production is excessive. The only viable option is to use contemporary satellite image analysis techniques in order to achieve estimates of biomass production at national level, and to calibrate and validate these by ground observation data.

NPP estimation from satellite images has been performed for many years and methods, algorithms and interpretations are well established in the literature. The basic of these techniques is a relationship between the amount of photosynthetic activity and the fraction of incoming radiation used by the plant cover to drive the photosynthesis. This will be described in more detail in the following section.

Estimation of NPP using satellite images is highly dependent on two factors: First the satellite sensor must record the amount of reflected radiation in suitable wavelength intervals, including the near-infrared. Second, the sensor should provide as frequent recordings of the surface in question as possible at as high a spatial resolution as possible. This limits the number of satellite/sensor systems useful for the purpose. The workhorse of NPP estimation for decades has been the AVHRR sensor onboard the NOAA satellite series. This sensor has provided reliable and consistent data for all of the globe since the mid 70’s with one daytime and one night

time observation per day. AVHRR images have a spatial resolution of 1.1 km at nadir.

Today, several satellite/sensor systems are available that share many of the attractive characteristics of the AVHRR sensor. The most obvious alternative is the MODIS sensor onboard the AQUA and TERRA satellite systems. These two satellites orbit the Earth at the same frequency as the NOAA series of satellite and provide daily coverage of almost the entire globe. The spatial resolution varies from 250 meter to 1000 meter depending on the spectral bands in question.

The vast majority of Earth Observation systems, including the AVHRR and MODIS, measure reflected sunlight in the near-infrared and in the red parts of the spectrum. The information obtained can be combined into a 'vegetation index', which is a good proxy for photosynthetic activity on the ground. There are several alternative 'vegetation indices', yet the most widely used is the 'normalized difference vegetation index', NDVI, calculated as

$$\text{NDVI} = \frac{\text{NIR} - \text{RED}}{\text{NIR} + \text{RED}}$$

In the formula NIR refers to the surface's reflectance factor (the fraction of the incoming radiation in the wavelength interval in questions which is reflected back) in the near-infrared and RED refers to the surface's reflectance factor in the red part of the spectrum.

In order to convert the daily observations of NDVI to an annual NPP estimate several steps need to be taken. First, NDVI is summed up for the entire length of the growing season. This results in a measure often referred to as iNDVI (integrated NDVI). The growing season may vary substantially between crops, rainfed and grazed, natural grassland and woodlands within Mali as a whole, and therefore the method used here involves integration over the whole year. Following the calculation of iNDVI this has to be converted into a measure of net primary production, using biome-specific relations. We have relied on the standard conversion methods, since we have insufficient ground data on NPP in Mali to develop a locally adapted model.

Several aspects of satellite derived estimates of NPP have to be taken into consideration when this type of data is employed in more detailed studies. Not least in relation to estimations of potentials for biomass production for energy purposes. These include:

- The results represent an average estimate of NPP within a given pixel. This estimate is however made up of contributions from several different surface types. A good example of this is the outskirts of the Mopti delta area on the Niger River, shown in figure 2.7. Here, the crop and vegetation cover is very inhomogeneous within the pixel, and the estimated NPP will be an average for all land use types within the pixel, including both relatively barren surfaces and lush irrigated areas. This implies that in areas such as the inland delta, the satellite-based estimates of NPP on a pixel basis may be relatively moderate, yet at the sub-pixel scale of individual, irrigated plots quite high NPP-values are likely to exist.
- NPP estimates based on remote sensing data and the methods described above are known to be biased for areas with high tree canopy cover. This implies that the results should be interpreted cautiously, especially in southern Mali.

As mentioned elsewhere in the report, it is important to note that while NPP is a measure of the total amount of biomass produced during the growing season, not all of this biomass will be available for energy purposes. The assessment of the fractions of NPP which are either harvested (for use as food, fibre or for 'conventional' fuel purposes), grazed or burnt (in controlled or uncontrolled fires) is very difficult, and this report only contains limited data on this issue.

In order further to qualify the analysis, NPP estimates were coupled with a land cover classification. In this case the GLC2000 (Global Land Cover) (Bartholomé & Belward, 2005) was used. The GLC2000 was produced by numerous research institutions collaborating on the production of a superior land cover classification. It is based on images from the SPOT-4 VEGETATION satellite /sensor system. The GLC2000 consists of a global coverage of land cover types and classifies the globe into 27 different land cover classes. The land cover classes used in the GLC are compatible with the FAO Land Cover Classification System (LCCS). Only 15 of these classes are present in Mali. These 15 classes were further agglomerated into 9 meaningful, functional classes, of which the 6 are relevant in the current context. The underlying assumption behind this approach is that it will be possible, for each of these classes, to discuss existing uses and demands for biomass, and as data becomes available, to assess the fractions of the NPP harvested, grazed and burnt. The reclassification of the GLC2000 is summarized in the table 3.1.

| | |
|---|---|
| Deciduous woodland | Deciduous woodland |
| Deciduous shrub land with sparse trees | Deciduous shrub land with sparse trees |
| Closed grassland | Grasslands types |
| Open grassland with sparse shrubs | |
| Open grassland | |
| Sparse grassland | |
| Croplands (>50%) | Croplands (>50%) |
| Irrigated croplands | Irrigated croplands |
| Croplands with open woody vegetation | Croplands with open woody vegetation |
| Sandy desert and dunes | Desert types |
| Stony desert | |
| Bare rock | |
| Water bodies | Water bodies |
| Cities | Cities |

*Table 3.1: The land cover classes used in this study. The left column shows the land cover classes present in Mali, the right column the agglomerated classes, of which the 6 first are used here.*

The classes may be briefly described as follows:

**Deciduous woodland** is only found in the extreme south of Mali and constitutes a very small fraction of the total land cover of Mali. It has been included in this analysis because it is functionally different from the other classes in that tree cover is abundant, interspersed with agriculture. It is assumed that the agricultural land use intensity in this land cover class is relatively low. Fires may be expected to consume a substantial part of the biomass.

**Deciduous shrub lands with sparse trees.** This land cover class is a dominant cover class for Kayes and Sikasso and while the name does not indicate it, wide spread agricultural activity must be assumed. Trees are present and form an integrated part of the agricultural landscape. The agricultural intensity is generally relatively high.

**Grassland types.** This category is a combination of several distinct cover types from the GLC2000, namely 'closed grassland', 'open grassland' with 'sparse shrubs', 'open grassland' and 'sparse grassland'. They have been added to form one functional unit for this study because their role in agricultural practices must be assumed more or less the same. In this land cover type we estimate that population density is very low and that the major agricultural activity is pastoralism. Also, we assume that the biomass produced during the brief rainy season is intensively grazed.

**Irrigated croplands.** Irrigated croplands are mainly located along the River Niger and in the large inland delta around Mopti. It has been included in this analysis since it may be relevant as a supplier of agricultural waste, potentially useful for energy purposes. The class is also interesting since it is densely populated and a local, established demand for power may be assumed to exist.

**Croplands and croplands with open woody vegetation.** While these two classes are treated separately in the following analysis they nevertheless resemble each other. The class is characterized by a very high intensity of agricultural land use with cotton, maize, millet and sorghum as the dominant crops. Considerable concentrations of different types of residues may be assumed to exist, and there is likely to be a local power demand. The extent to which residues are used for other purposes, such as livestock fodder, is unknown.

**Desert types, water bodies and cities**. These three classes are excluded from the analysis for obvious reasons.

## 4.5 Results

### 4.5.1 NPP

The NPP map, produced on the basis of MODIS data by means of the methods described above for the year 2006, is shown I figure 3.1.

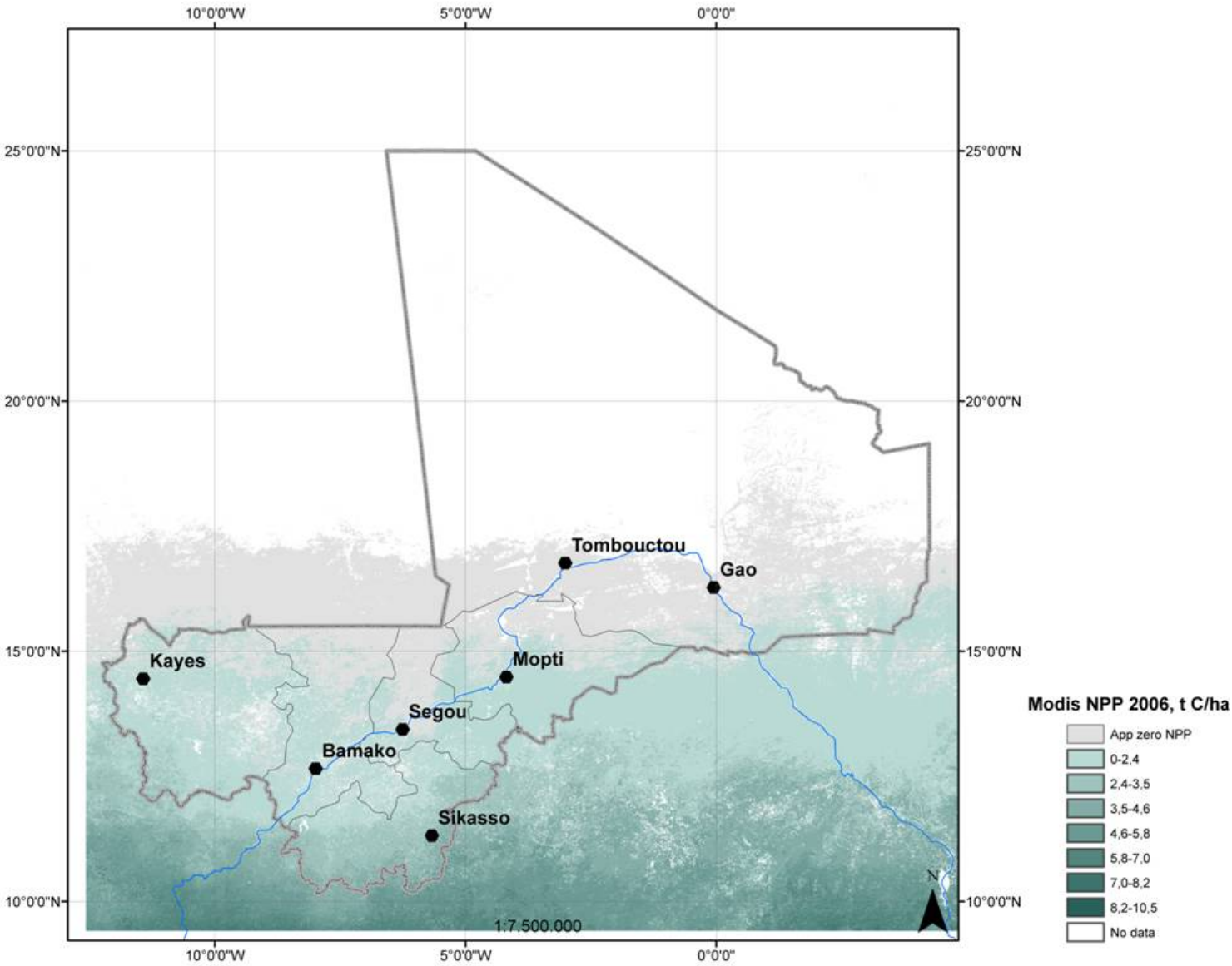


*Figure 3.1: MODIS NPP 2006*

Average NPP, as estimated using MODIS data for the year 2006, for each of the surface cover types is illustrated in figure 3.2. Note that the numbers given can be converted into dry matter by multiplying by a factor 2. Also, a map is supplied illustrating the spatial distribution of the observed NPP.

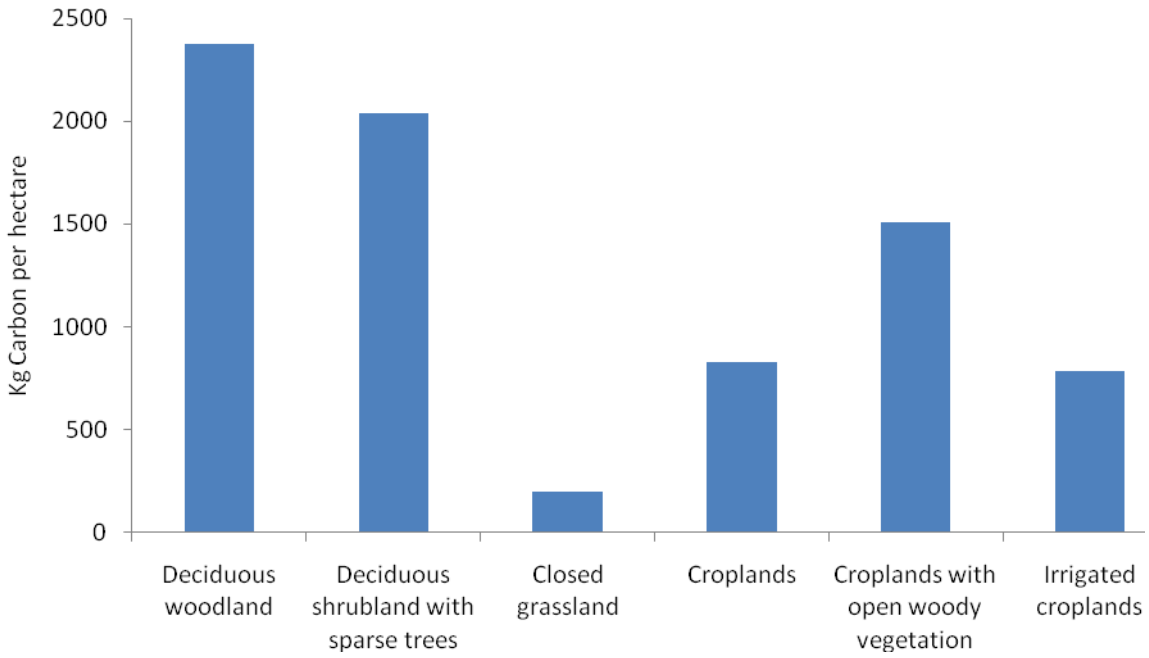


*Figure 3.2: NPP, estimated from MODIS, for the 6 GLC2000 land cover classes. Note that the y-axis shows the mass of carbon, and not dry matter, stored in the above ground vegetation.*

As it is readily seen, the deciduous woodland class exhibits the highest production of vegetation with the shrubland class as the second highest. However, it is worthwhile to note that the deciduous woodland class covers less than 10% of the area of any of the other classes, except for the irrigated croplands. Also, it should be noted that much of the observed NPP for the woodland and shrubland classes will be produced by woody vegetation. Since this production is partly harvested in forestry and to a great extent used as fuel wood, it is not available for other energy uses without losses in traditional uses.

The 'irrigated croplands' class has a surprisingly low average NPP. As we will return to later, the explanation is that the surface cover is extremely heterogeneous at sub-pixel-scale, with very high NPP plots, e.g. rice fields, interspersed with barren ground and water. Seen from a bio-fuel perspectives such areas might be quite interesting, in spite of the low average NPP, since the production is concentrated on small areas. This will allow efficient and inexpensive harvesting of agricultural residues.

It may be concluded that the observed NPP is relatively low for large parts of Mali. The figure given for the grassland class is lower, than most other estimates, however, and it may be questioned if the iNDVI-to-NPP conversion is giving rise to a general underestimation at the low end of the scale. Further it should be noted that within these very broad land cover classes much variation can be found, as illustrated in figure 3.3, illustrating the within-class variability at pixel scale. While the mid-points of figure 3.3 corresponds to the bars of figure 3.2 the vertical lines illustrates the variance around the average. In this case only the most commonly found 25 percent is illustrated (corresponding to the average value ± 0.34 standard deviations). From this graph it is apparent that both of the two high scoring surface cover types also have a very large spatial variability, presumably caused by a very heterogeneous - mixture of surface types at micro-scale. The grasslands class on the other hand shows only a very limited spatial variation.

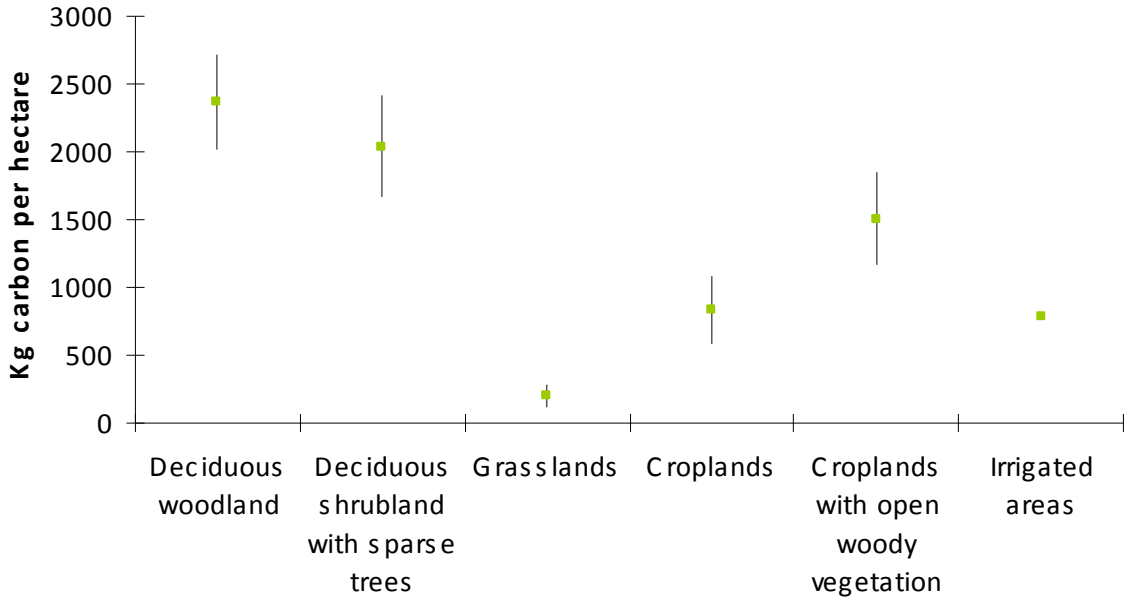


*Figure 3.3: Average values and deviations for MODIS NPP (in kg C/ha*year) segmented by GLC2000 land cover classes. Note that deviations are given as the most common 25% of the results in a given land cover class*

Still, the most obvious conclusion from the above two graphs is that only in the southernmost land cover classes that contain some amount of woody vegetation does the average net above ground primary production seem to exceed an average level of 1 ton of carbon per hectare (above ground). This will seriously limit the spatial domain in which there is a high potential for bio-energy production.

These points are further illustrated in the below table 3.2. Here the underlying statistics for figure 3.3 are displayed.

| NPP in kg C/(ha*year) | **Deciduous woodland** | **Deciduous shrubland with trees** | **Grassland** | **Cropland** | **Croplands with woody vegetation** | **Irrigated areas** |
|---|---|---|---|---|---|---|
| Max NPP | 5064 | 7179 | 2174 | 3529 | 6356 | 4089 |
| Upper quartile NPP | 2722 | 2412 | 277 | 1076 | 1854 | 785 |
| Average NPP | 2373 | 2038 | 197 | 828 | 1508 | |
| Lower quartile NPP | 2023 | 1665 | 117 | 580 | 1162 | |

*Table 3.2: NPP (max, upper quartile, average and lower quartile) for six land cover classes*

From inspection of table 3.2 it is found that while the deciduous woodland class has the highest average value it is actually the deciduous shrublands with trees that contains the highest maximum NPP of more than 7 t C/ha. Even more interesting is the fact that the croplands with woody vegetation show a maximum production for 2006 of more than 6.3 t C/ha. It is clear from the table that the distributions are skewed, implying that a few pixels have NPP values several times higher than the average.

Another issue of importance when planning bio-energy production is the temporal variability. The Sahel-Sudan zone is well-known for great rainfall variability, and basing a renewable energy system on biomass-resources which are extremely variable in amount from year to year is obviously irrational. In figure 3.4 is shown to temporal variability of iNDVI for four points in Mali. These four areas will be returned to later in the discussion of 'case studies'. The temporal variation has been derived from a study based on use of NOAA AVHRR data from the Global Inventory Modeling and Mapping Studies (GIMMS) (see also http://gimms.gsfc.nasa.gov/) with a (degraded) spatial resolution of around 8*8 $km^2$, and thus the numbers are not directly comparable to the iNDVI values from the MODIS analysis.

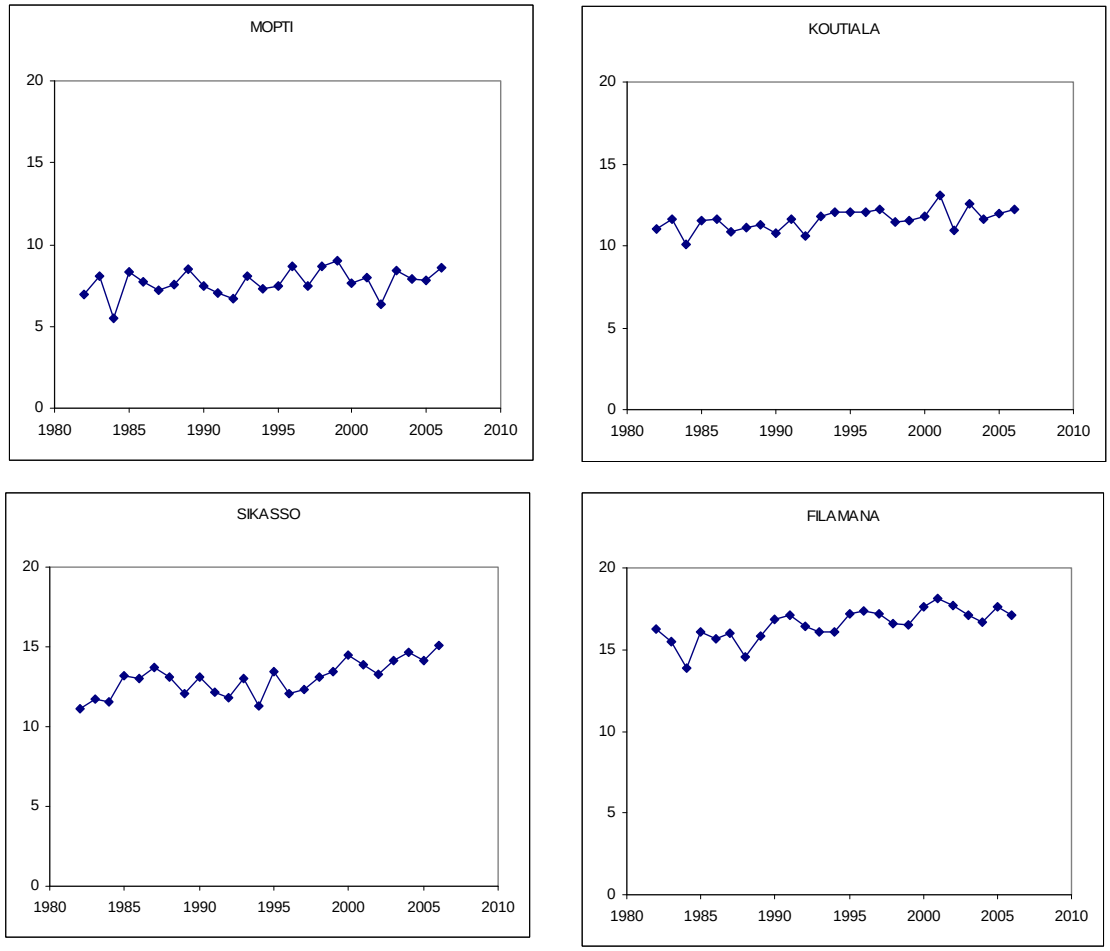


*Figure 3.4: Temporal variation of iNDVI for four areas in Mali for the period 1982-2007*

It is clear from figure 3.4, that both the absolute and the relative sizes of the variability are greatest furthest to the North, in Mopti. The reason for the higher variability may both be that the rainfall itself varies more to the North, and that the NPP is also more sensitive to rainfall variations in the North, as also noted earlier. There is the further complication that part of the iNDVI signal in the North derives from irrigated fields, the area and greenness of which depend on the river discharge, which reflects rainfall conditions in the Fouta Djalon. These may differ substantially from local conditions. Climate change is likely to increase variability in the future.

In figure 3.5 NPP is shown for each district in Mali. Also included in the figure is the Coefficient of Variance. The coefficient of variance is the ratio of the spatial standard deviation to the average value. In the figure it is noteworthy that only two of the districts in Mali exhibit NPP levels above 1 ton per hectare, namely Kayes and Sikasso. At the same time, these two provinces have the lowest values of variance. Bamako and Segou are more or less of the same magnitude, while Gao and Mopti scores lowest. Mopti province also has the highest level of variance which is a direct consequence of the large inland delta situated in the middle of a relatively barren area.

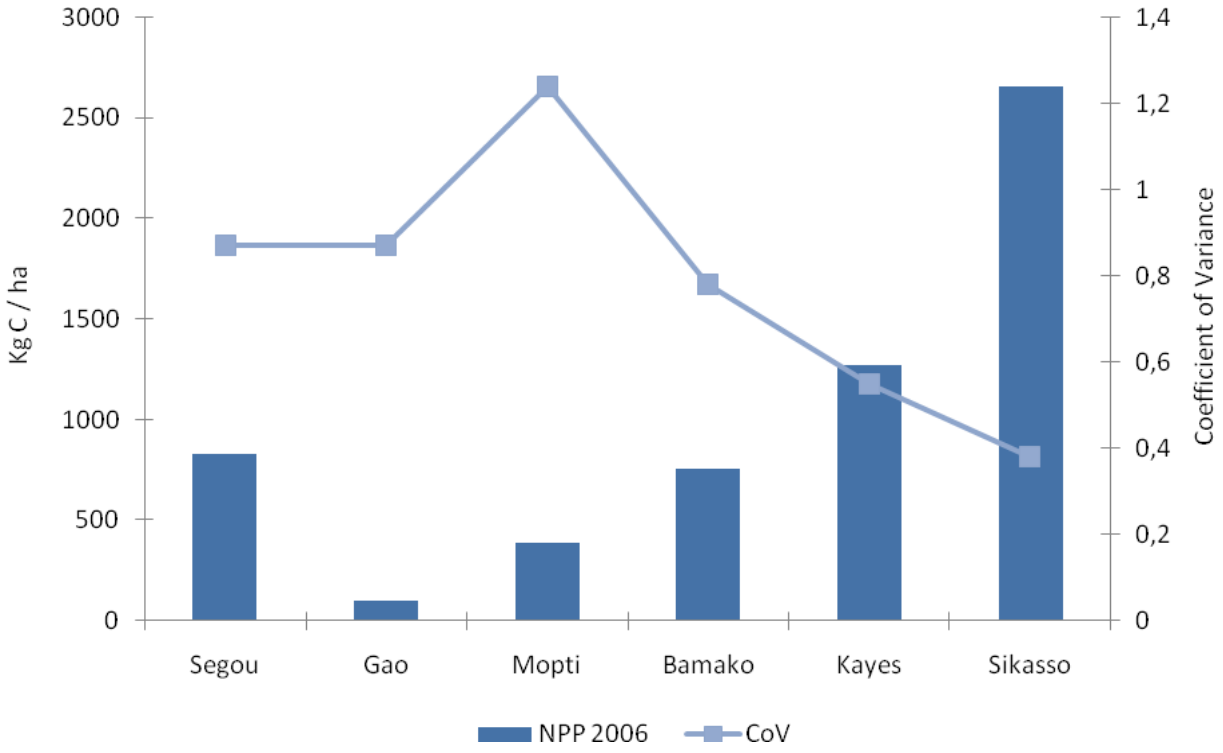


*Figure 3.5 MODIS NPP and Coefficient of Variance for the 6 provinces of Mali. Bars illustrate NPP while the line shows the CoV.*

It is obvious that the distribution of NPP in the 6 provinces of Mali is closely linked to the physical characteristics of each of the provinces. It would be expected that Gao scores much lower on NPP than Bamako or Sikasso. If figure 3.5 is juxtaposed to information on the fraction of the various land cover classes this becomes even more evident, as shown in table 3.3. In table 3.3 the fractions of each of the GLC2000 land cover classes are listed for each of the provinces in Mali. Generally speaking, and as can be found in the graph in figure 3.5 the provinces can be divided into three: The Northern provinces of Gao and Mopti where land cover is dominated by desert types and by the vast grasslands. Next are the central provinces of Segou and Bamako. Here NPP is generally low with average amounts of carbon in NPP for 2006 less than 1 ton per hectare. At the same time, these two provinces are the two provinces where agriculture is most commonly found with approximately three quarters of the total area occupied by agriculture with varying degrees of tree cover. Finally, the two provinces of Kayes and Sikasso exhibit the highest levels of NPP for

2006. These are also the two provinces where land cover is dominated by tree cover in one form or another. More than 75% of the total area of these provinces is occupied by the following classes: *croplands with woody vegetation, deciduous woodlands and deciduous shrublands with trees.*

| Distribution in percent | **Segou** | **Gao** | **Mopti** | **Bamako** | **Kayes** | **Sikasso** |
|---|---|---|---|---|---|---|
| Grasslands | 26 | 14 | 72 | 13 | 2 | 0 |
| Croplands | 64 | 0 | 19 | 38 | 23 | 14 |
| Croplands with woody vegetation | 8 | 0 | 2 | 38 | 32 | 38 |
| Irrigated areas | 1 | 0 | 7 | 0 | 0 | 0 |
| Deciduous woodland | 0 | 0 | 0 | 0 | 4 | 3 |
| Deciduous shrubland with trees | 0 | 0 | 0 | 11 | 39 | 45 |
| Desert types | 0 | 86 | 1 | 0 | 0 | 0 |
| Total | 100 | 100 | 100 | 100 | 100 | 100 |

*Table 3.3: The distributions of the 7 land cover classes over the 6 districts of Mali*

The spatial distribution of agglomerated GLC2000 land cover classes is shown in figure 3.6. Large parts of the country are not part of this analysis. The criteria for excluding areas have been the following:

- Due to the high quality demand for the MODIS data used in the calculation of NPP, many pixels are removed from the analysis. Most frequently this is due to persistent cloud cover in the growing season of 2006,
- All pixels with iNDVI-values below a certain threshold, representing so little NPP that they are considered not interesting from a bio-energy point of view, are excluded.
- All GLC2000 desert land cover types are effectively excluded from this analysis since they are not either considered interesting as a basis for the production of bio-energy.
- Finally, some pixels can be excluded from the analysis if they are marked as low quality pixels in the MODIS NPP product.

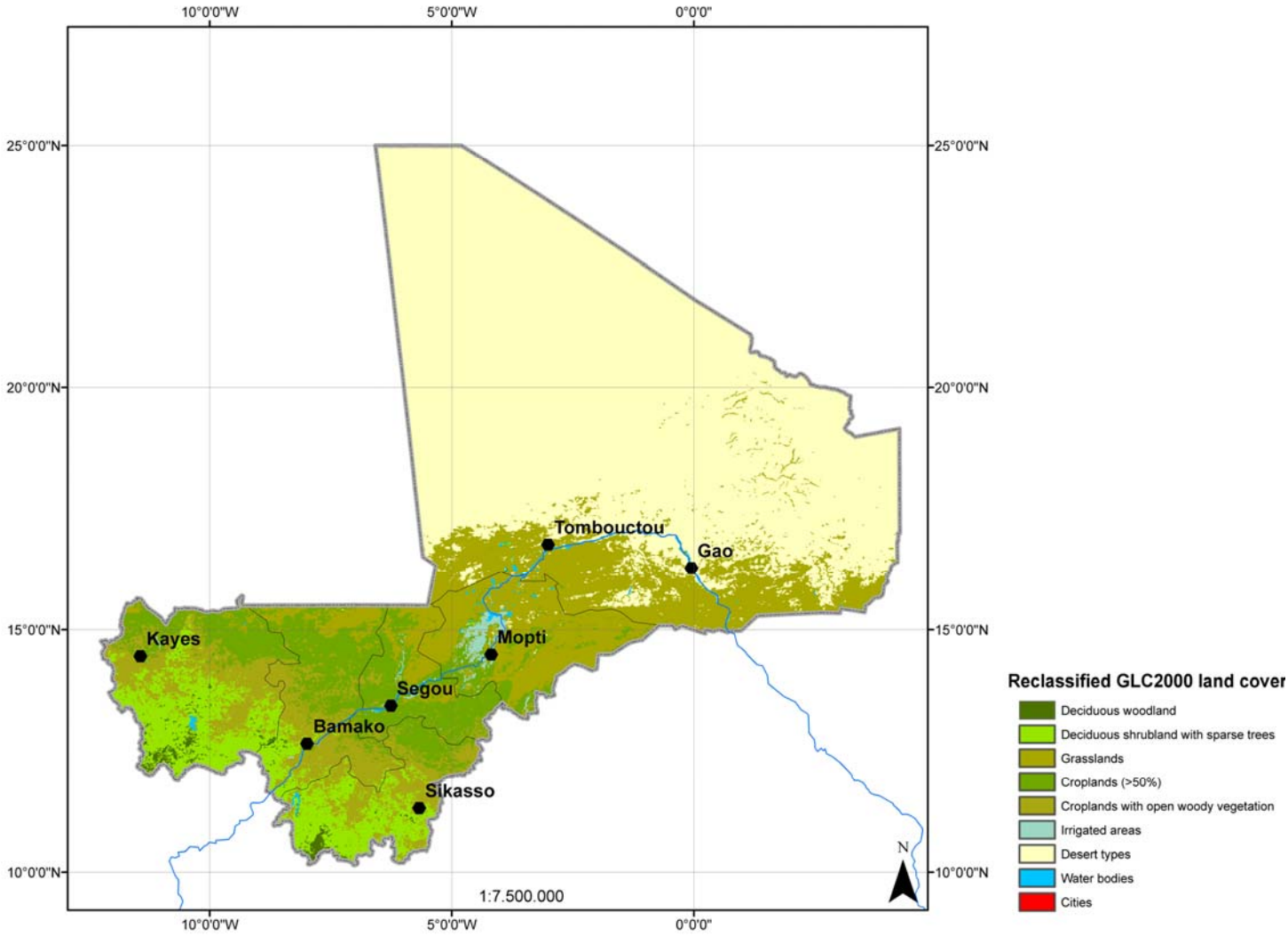


*Figure 3.6: Reclassified GLC2000 land cover map (see also table 3.1)*

In order to analyze in more detail the information contained in the combination of the NPP and land cover maps, the land cover classes have been segmented in three, according to the NPP-level: Each of the land cover classes of interest were divided into three subclasses based on the average values and standard deviations of NPP, as shown in figure 3.2. Hence, each land cover class was divided into three classes: A high, medium and low NPP land cover class. This resulted in 15 classes plus one class; irrigated areas, which was not segmented further due to its small size. The results are shown in table 3.4.

| NPP (tons C per hectare) | Low | Middle | High |
|---|---|---|---|
| Deciduous woodland | [1,15; 1,77] | [2,24; 2,52] | [3,02; 3,71] |
| Deciduous shrubland with trees | [0,74; 1,39] | [1,77; 2,21] | [2,73; 3,71] |
| Grassland | [0,03; 0,14] | [0,13; 0,24] | [0,28; 0,73] |
| Cropland | [0,14; 0,63] | [0,7; 0,92] | [1,27; 2,16] |
| Croplands with woody vegetation | [0,46; 0,91] | [1,29; 1,63] | [1,98; 3,10] |
| Irrigated areas | [0,35;1,22] | | |

*Table 3.4: NPP for each of the segmented GLC land cover classes. The interval shows the range of NPP estimates corresponding to the mean value plus/minus 0.67 standard deviations. This is the interval within which 50 % of all observations are to be found, assuming a normal distribution.*

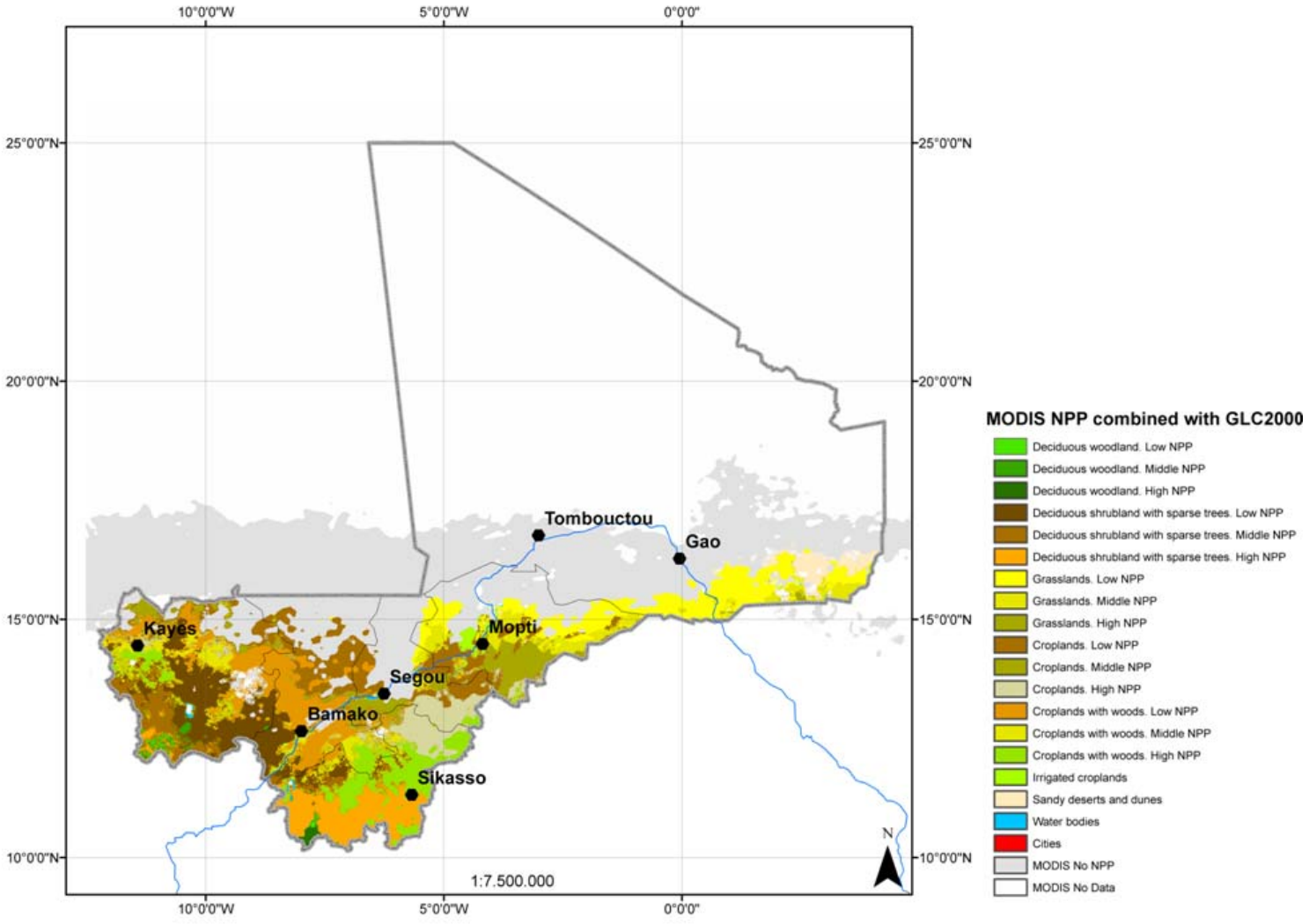


*Figure 3.7: The GLC2000/NPP combined map*

Table 3.4 should be seen in close connection with figure 3.7 where the spatial extent and location of each of these classes can be seen. From the perspective of potential areas for the production of various energy crops it seems reasonable to prefer areas with a high production of NPP.

### 4.5.2 The fraction of NPP available for bio-energy

Very little information is available at the national level as concerns the fractions of the NPP harvested, grazed and burnt. The following general trends may be suggested on the basis of common knowledge of agriculture and environment in the Sahel zone, mainly derived from experience from Senegal:

The harvested biomass includes agricultural crops and forestry products. The extent of crop cultivation in Mali may be derived from FAO statistics, both the areas cultivated with different crops and the yields obtained. We will disregard the crops themselves, assuming that they will continue to be used mainly for the purposes they are presently cultivated, yet crop residues are potentially interesting. Many of them can not at present be used for production of bio-ethanol, but this may change as 2nd Generation technologies become available. Some of the residues may, after drying, be used as fuel in conventional power plants. Some of the potentially most important crop residues derive from cotton, rice, maize and sorghum, and residues constitute of 45 – 70% of the total dry matter produced. Figures from The Mopti area indicate that approximately 1.200 kg/(ha*year) of residues are produced in cotton fields, while the corresponding figures for maize, sorghum and millet are approximately 3000, 5100 and 5700 kg/(ha*year). These estimates are based on a count of the number of '*charette*' loads of residues per ha and the weight per load. While the figures appear great, compared to the NPP figures presented above, it should be noted that they need to be corrected for water content and divided by a factor of 2 to translate them into figures comparable to the carbon figures given. In addition, they may represent atypical circumstances and above-average application of inputs, including fertilizers and irrigation. However, these figures may well indicate the potential, as higher inputs will become increasingly realistic when prices of bio-energy feedstock increase. Field observations indicate that all types of agricultural residues are presently being used as animal fodder, and stems and leaves from maize, sorghum and millet are used for mulching as well. Thus, at least in the Mopti area, any application of agricultural residues for energy purposes will have significant effects on other uses of residues, including the livestock production.

With respect to the forestry production, which is outside the scope of the present study, relatively little can be said about the unused resources. Production figures for forests are available, but these will not be discussed here.

With respect to the fraction of NPP consumed by grazing livestock, little quantitative information has been identified. In the rangelands of northern Mali, almost all biomass is expected to be consumed by grazing livestock in any 'normal' year, and livestock will either starve in the end of the dry season or be moved further south to graze stubble fields in the agricultural zone (thereby potentially competing directly with the use of agricultural residues for bio-energy purposes) or graze in the savannah woodlands of the southern Sudanian zone. It is therefore not realistic and socially sustainable to think in terms of utilizing the rangelands with bio-energy production. Anyway, the NPP of the northern rangelands is so low that it is hardly realistic to harvest it for bio-energy use, except for the seasonally flooded grasslands in the inland delta, which have high productivity. These grazing resources are, on the other hand, of key importance to pastoralists in the dry season, and the negative

effect on the pastoral production system of harvesting them will be great. In the southern parts of Mali, there may well be un-grazed herbaceous biomass resources, since the livestock density is less and NPP much higher. Much of the vegetation left in the dry season has very limited nutritional value to the livestock.

It is exactly in the southern savannah woodlands that the frequency and extent of biomass burning is highest, and the dry grasses and herbs left after the end of the rainy season constitutes a large part of the fuel load of these fires. If this biomass is used for bio-energy purposes, the impacts on the environment may be expected to be minimal, apart from the removal of a certain amount of plant nutrients, not the least phosphorous. We have no data indicating whether the harvesting of 'unused' biomass in these southern areas for bio-energy purposes is economically feasible.

Finally, it is, of course, worth considering whether it is realistic to convert areas in the south with relatively low current utilization intensity to cultivation of energy crops, be it *Jatropha carcus* for bio-diesel or cassava for bio-ethanol. While *Jatropha* is often proposed as a win-win option for use in degraded areas, it certainly produces far better in areas with high rainfall and with an ample supply of plant nutrients, yet little precise data on yields is available. Cassava, on the other hand, is a widespread, yet low-status food crop with a well-documented high yield potential, which may be used as feedstock, even with use of presently available 1st Generation technology. In-depth studies are required to assess the realism and sustainability of these options, including their impacts on local environments and livelihoods.

### 4.5.3 Selected study areas

As mentioned above, the coarse, national-scale analysis has been supplemented with a 'zoom-in' on areas of potential interest, seen from a bio-energy point of view. The basis for selecting these areas have been the following

- They should represent different GLC2000 land cover classes
- They should represent regions of a certain potential interest in a bio-energy context
- They should represent different situations with respect to alternative uses of biomass

We have selected the following four areas:

- Mopti, representing the inland delta with irrigated fields, mainly with rice, as well as seasonally flooded grasslands along with drylands with very low NPP
- Koutiala, representing a relatively intensively used cropland with few trees.
- Sikasso, representing a slightly more wooded agricultural area, with a mixture of land cover types, yet still quite intensively cultivated
- Filamana, representing woodland in the southernmost Mali, with a lower percentage cultivated area. This area may have a potential for producing cassava as a bio-ethanol feedstock.

These four areas will be briefly presented below, yet an assessment of their precise potentials as suppliers of bio-energy requires extensive field work, beyond what has been foreseen in this pilot project.

All the following images have been acquired from google.maps.com. The first three of them derive from either aerial photos or ultra-high resolution satellite/sensor

systems (such as Quickbird or IKONOS), yet the exact source is not known. The spatial resolution of these images is in the order of 0.6 – 2 m. and the sections shown cover few $km^2$. The last image, covering the Filamana area, is from LANDSAT TM and has a spatial resolution of 28.5 meter at nadir. Hence, the total size of the image is approximately 100 $km^2$.

*Study area 1, Mopti.*

The Niger inland delta attracts special attention due to the very high levels of biomass produced in seasonally flooded grasslands and in the irrigated areas. In the image in figure 3.8, parts of the city of Mopti can be seen along the banks of the river. On the western bank of the river to the South of Mopti, agricultural land use can not be observed. In sharp contrast to this, the eastern part of the image is dominated by numerous small, rectangular fields. These fields vary in colour and brightness, indicating that some of them have a crop cover while others are barren. Each of the fields are much smaller than the spatial resolution of the MODIS images, which clearly illustrates the limitations of NPP-estimation, derived from 1 $km^2$ pixels of the MODIS data, for an intensively cultivated area like this: All pixels will contain a mixture of fields in various stages of cultivation, including some which are flooded. If an average is taken over one year and over 1 $km^2$, as done in the present study, the result will not be very high, as discussed above. Nevertheless the agricultural residues from the irrigated rice fields may very well constitute a potential feedstock for bio-energy use, up to 10 t/ha dry matter has been recorded. The extent to which these residues are presently utilized, either as fuel or as fodder, is not known, however.

*Figure 3.8: Study area 1: Mopti*

*Study area 2: Koutiala*

In figure 3.9 a small section, covering few $km^2$, of the outskirts of Koutiala is shown. This area falls in the category of areas in the croplands class with a high level of NPP. The image is clearly acquired during the dry season and it is difficult to tell different types of surfaces apart. Still, it is clear that large parts of the areas north of the stream is under cultivation and that the fields are considerably larger and less regular in shape than was seen in Mopti. Also, some areas along the stream are clearly cultivated as fields, but may be used as garden areas for the production of vegetables, or as grazing. In the NW-corner, an area seems to be used for grazing, and is probably in fallow. Some trees are visible in the fields. It is likely that very little biomass is left unused in this area, and the potential for bio-energy is limited to a possible use of agricultural residues.

*Figure 3.9: Study area 2: Koutiala*

*Study area 3: Sikasso*

Figure 3.10 shows an image from the north western outskirts of Sikasso. This image is included as an example from the GLC2000 class 'croplands with woody vegetation'. In the image it is readily seen that trees are more abundant than was the case in the Koutila area and that trees are not only present in the form of scattered trees in and around the fields, but regular, small forests are also visible, including newly planted areas. Most of the area is intensively cultivated, with relatively large fields to the East, and smaller (and greener) fields with fewer trees to the West. Again, the bio-energy potential in this area must be expected to be associated with agricultural residues, and the extent to which these are being used for dry-season grazing is a critical factor.

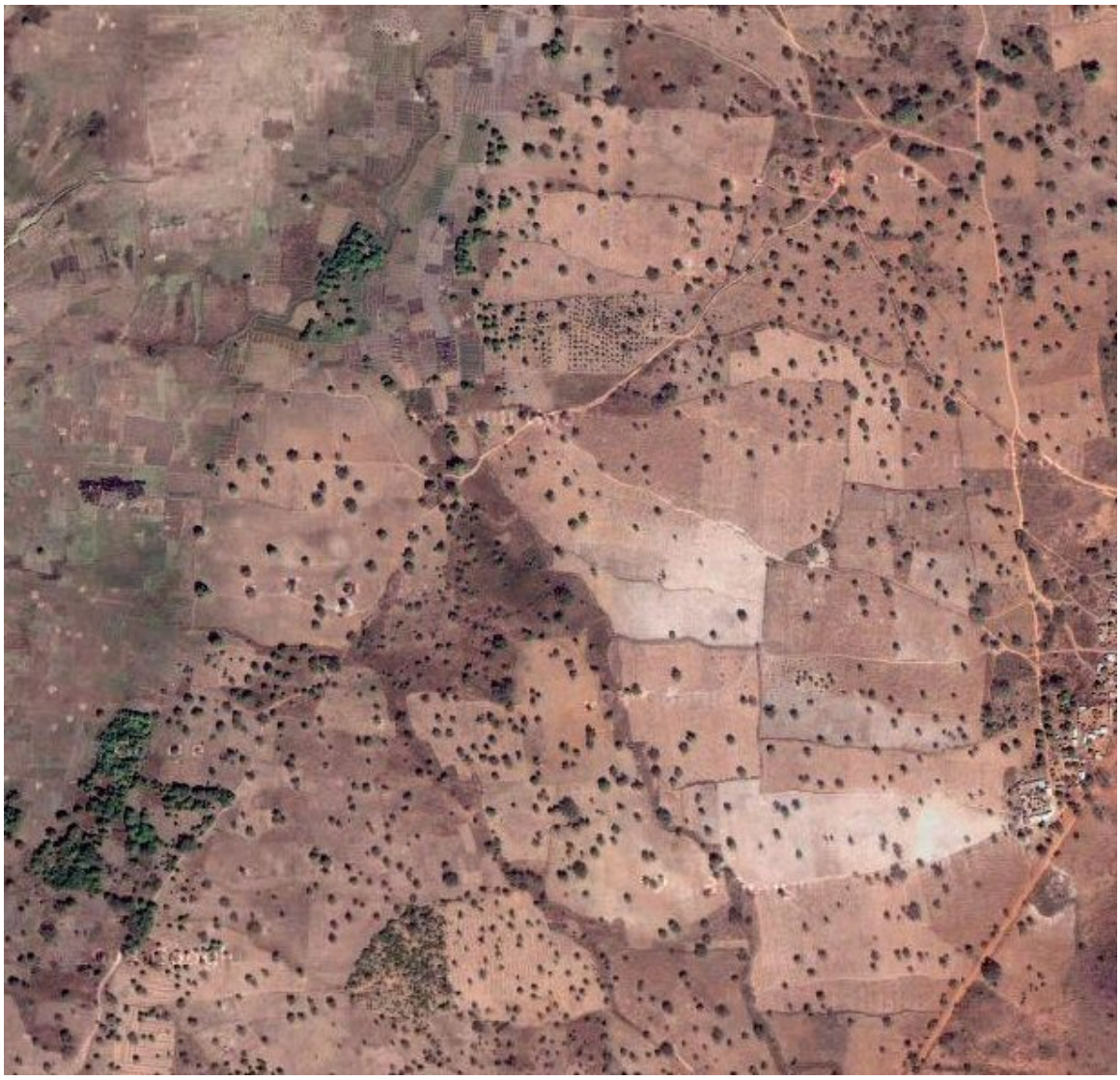

*Figure 3.10 Study area 3: Sikasso*

*Study-area 4: Filamana*

Figure 3.11 shows the area around Filamana in the South of Mali. This area was selected as a zone of interest due to the higher density of tree-cover, the lower agricultural land use intensity and the high NPP. It is located in the GLC2000 class of deciduous woodlands. The image above has a spatial resolution of 28 m, and covers approximately 100 $km^2$. In the lower right part of the image is the town of Filamana. Fields, identifiable on the basis of their brightness and regular shapes, may be seen scattered over the image, yet the area cultivated does not exceed 20 %. Large areas of woodland may be identified, and some of them show signs of burning. The area is likely to have a relatively high potential as a supplier of bio-energy, both herbaceous and woody vegetation, and land conversion to production of energy crops may also be realistic.

*Figure 3.11: Study area 4: Filamana2.6*

## 4.6 Discussion and conclusions

The results shown clearly demonstrate that Mali has an extremely uneven distribution of NPP. Since a certain minimum NPP is required in order to have a sufficiently spatially concentrated supply of biomass for energy applications, only southern Mali is relevant. Two exceptions from this rule should be mentioned:

Firstly, the irrigated agricultural area in the inland delta has a high production on a relative small area, and agricultural residues (and especially rice straw) are produced in concentrations making them a relevant biomass source. Secondly, *Jatropha carcus* may be cultivated with reasonable yields even in relatively dry areas, providing a source of plant oil which may substitute diesel.

The temporal distribution of NPP is (apart from the irrigated areas) determined by the rainy season. Some of the biomass may, however, be harvested all year or through extended periods of the year. This is true for woody material, for dry grasses and straw, for fruits from *Jatropha*, and for root crops such as cassava. This is a clear advantage in terms of assuring a steady supply for bio-fuel production and/or combustion in power plants.

Further, our data shows that much of the biomass produced is either harvested for human consumption, grazed by or used as fodder for livestock, or burned in uncontrolled fires. Future use of biomass, presently used for human consumption or animal fodder, for energy purposes will have costs, and careful weighting of benefits and costs is required. Biomass presently burned may alternatively be used for energy purposes at limited cost, yet this presumes that burning can be reduced, which may be quite difficult to achieve. Further, such reduction in burning is likely to have certain side-effects on ecosystem function, and these effects need to be studied before steps are taken in this direction.

It is clear from our data that the fraction of the biomass which is available for energy purposes with small negative impacts on other production systems and the environment is greatest in the far South, where a smaller fraction is consumed by livestock. Other areas where this available fraction is relatively high may be rice production areas and cotton areas, where a substantial amount of residues are burnt. These residues may be a potentially interesting feedstock for bio-ethanol production as 2$^{nd}$ Generation technologies become available.

In conclusion it may be stated that the greatest potentials, presently and within a few years, of using biomass in the energy system of Mali are the following:

- Cultivation of *Jatropha carcus* for plant oil production.
- Production of cassava as feedstock for bio-ethanol production in areas of southern Mali with suitable climatic conditions and soils and currently characterized by low-intensity land uses.
- Use of concentrations of agricultural residues, e.g. in rice growing areas in the inland delta, and in cotton areas, for combustion in decentral power plants and/or as feedstock for bio-ethanol production using 2$^{nd}$ generation technologies.
- Use of woody material and residues from forestry, mostly in the southern part of Mali, for combustion in local power plants and/or as feedstock for bio-ethanol production using 2$^{nd}$ generation technologies.

Apart from these potentials, in much of Mali NPP is too low and biomass too intensively used for livestock grazing/fodder to allow for an economically efficient application for energy purposes. However, this assessment is preliminary, based on limited data, and more intensive *in situ* studies are required, including also an economic assessment of the economic rationale of basing an energy system on biomass resources.

# 5 References

MMEE, 2007. Stratégie Nationale pour le développement des Energies Renouvelables. Bamako: Ministère des Mines, de l'Energie et de l'Eau (MMEE)

## Chapter 1, Wind Assessment

Adrian, G, 1994. Zur Dynamik des Windfeldes über orographisch gegliedertem Gelände, Ber Deutschen Wettedienstes 188, Offenbach am Main 1994, 142 pp.

Adrian, G., F. Fiedler, 1991: Simulation of unstationary wind and temperature fields over complex terrain and comparison with observations. *Beitr. Phys. Atmosph*., 64:27-48

Frank, H. P., L. Landberg, 1997. Modelling the wind climate of Ireland. *Boundary-Layer Meteorology*, 85:359-378

Frank, H. P., O. Rathmann, N. G. Mortensen, L. Landberg, 2001: The Numerical Wind Atlas – the KAMM/WAsP Method, Risoe National Laboratory, Roskilde, Denmark. ISBN 87-550-2850-0, Risø-R-1252(EN).

Frank, H. P., L. Landberg, 1997. Modelling the wind climate of Ireland. Boundary-Layer Meteorology, 85:359-378

Frey-Buness, F., D. Heimann, R. Sausen, 1995. A statistical-dynamical downscaling procedure for global climate simulations. *Theor. Appl. Climatol*., 50:117-131

Kalnay E, Kanamitsou M, Kistler R, Collins W, Deaven D, Gandin L, Irebell M, Saha S, White G, Woollen J, Zhu Y, Leetmaa A, Reynolds R, Chelliah M, Ebisuzaki W, Huggins W, Janowiak J, Mo KC, Ropelewski C, Wang J, Jenne R, Joseph D, 1996. The NCEP/NCAR 40-year reanalysis project. *Bulletin of the American Meteorological Society* **77**: 437-471

Klemp, J.B., D.R. Durran, 1983. An upper boundary condition permitting internal gravity wave radiation in numerical mesoscale models. Mon. Wea. Rev. 1983, 111, 430-444.

Mortensen, N.G., J.C. Hansen, J. Badger, B.H. Jørgensen, C.B. Hasager, L. Georgy Youssef, U. Said Said, A. Abd El-Salam Moussa, M. Akmal Mahmoud, A. El Sayed Yousef, A. Mahmoud Awad, M. Abd-El Raheem Ahmed, M. A.M. Sayed, M. Hussein Korany, M. Abd-El Baky Tarad, 2005. Wind Atlas for Egypt, Measurements and Modelling 1991-2005. New and Renewable Energy Authority, Egyptian Meteorological Authority and Risø National Laboratory. ISBN 87-550-3493-4. 258 pp.

Mortensen, N.G., D.N. Heathfield, L. Myllerup, L. Landberg and O. Rathmann (2007). Wind Atlas Analysis and Application Program: WAsP 9 Help Facility. Risø National Laboratory, Technical University of Denmark, Roskilde, Denmark. 353 topics. ISBN 978-87-550-3607-9.

Troen, I., E. L. Petersen, 1989. European Wind Atlas. Risø National Laboratory for the Commission of the European Communities, Roskilde, Denmark, ISBN 87-550-1482-8.

### Internet links

[1] ftp://e0srp01u.ecs.nasa.gov

[2] http://edcsns17.cr.usgs.gov/glcc/

[3] http://www.cdc.noaa.gov/cdc/reanalysis/

## Chapter 2 and 3, Solar and biomass assessment


Bartholomé, E. & Belward, A. (2005) GLC2000: a new approach to global land cover mapping from Earth observation data. International Journal of Remote Sensing Vol. 26, No. 9, 10 May 2005, 1959–1977

Beyer, H. G., Costanzo, C., & Heinemann, D. (1996). Modifications of the Heliosat procedure for irradiance estimates from satellite images. Solar Energy, 56, 207-212.

Cano, D., Monget, J. M., Albuisson, M., Guillard, H., Regas, N., & Wald, L. (1986). A Method for the Determination of the Global Solar-Radiation from Meteorological Satellite Data. Solar Energy, 37, 31-39.

Christensen, J.H., B. Hewitson, A. Busuioc, A. Chen,X.Gao, I.Held, R. Jones, R.K. Kolli,W.-T. Kwon, R. Laprise, V.Magaña Rueda, L. Mearns, C.G. Menendez, J. Räisänen, A. Rinke, A. Sarr and P. Whetton, (2007). Regional climate projections. In: Climate Change 2007: The Physical Science Basis. Contribution of Working Group I to the Fourth Assessment Report of the Intergovernmental Panel on Climate Change, S. Solomon, D. Qin, M. Manning, Z. Chen, M. Marquis, K.B. Averyt, M. Tignor and H.L. Miller, Eds., Cambridge University Press, Cambridge and New York, 847-940.

Diabaté, L., Demarcq, H., Michaud-Regas, N., & Wald, L. (1988). Estimating Incident Solar Radiation at the Surface from Images of the Earth Transmitted by Geostationary Satellites: the Heliosat Project. International Journal of Solar Energy, 5, 261-278.

Gautier, C., Diak, G., & Masse, S. (1980). A Simple Physical Model to Estimate Incident Solar-Radiation at the Surface from Goes Satellite Data. Journal of Applied Meteorology, 19, 1005-1012.

Ineichen, P. & Perez, R. (2002). A new airmass independent formulation for the Linke turbidity coefficient. Solar Energy, 73, 151-157.

Iqbal, M. (1983). An Introduction to Solar Radiation. 1-387.

Möser, W. & Raschke, E. (1983). Mapping of Global Radiation and of Cloudiness from Meteosat Image Data -Theory and Ground Truth Comparisons. Meteorologische Rundschau, 36, 33-41.

Möser, W. & Raschke, E. (1984). Incident Solar-Radiation Over Europe Estimated from Meteosat Data. Journal of Climate and Applied Meteorology, 23, 166-170.

Stisen, S. (2007): Geostationary Remote Sensing in Modelling of Land Surface Hydrology. Ph.D Thesis, University of Copenhagen (http://www.fiva.dk/doc/thesis/PhD_Thesis_Simon_Stisen.pdf)

SoDa (2007). Website of the The SoDa Service for Knowledge in Solar Radiation. http://www.soda-is.com/eng/index.htmlMarch 2007.

Stewart, J. B., Watts, C. J., Rodriguez, J. C., de Bruin, H. A. R., van den Berg, A. R., & Garatuza-Payan, J. (1999). Use of satellite data to estimate radiation and evaporation for northwest Mexico. Agricultural Water Management, 38, 181-193.

Stuhlmann, R., Rieland, M., & Raschke, E. (1990). An Improvement of the IGMK Model to Derive Total and Diffuse Solar-Radiation at the Surface from Satellite Data. Journal of Applied Meteorology, 29, 586-603.

Tarpley, J. D. (1979). Estimating Incident Solar-Radiation at the Surface from Geostationary Satellite Data. Journal of Applied Meteorology, 18, 1172-1181.

Tuzet, A., Möser, W., & Raschke, E. (1984). Estimating Global Solar Radiation at the Surface from METEOSAT-data in the Sahel Region. Journal de Recherches Atmosphériques, 18, 31-39.

# 6 Appendix

**Appendix A:**
Month average solar radiation values (Wh/m2/day)

**Appendix B:**
Evaluation des ressources de la biomasse agricole et de sa valorisation énergétique au Mali

## Appendix A – Month average solar radiation values (Wh/m$^2$/day)

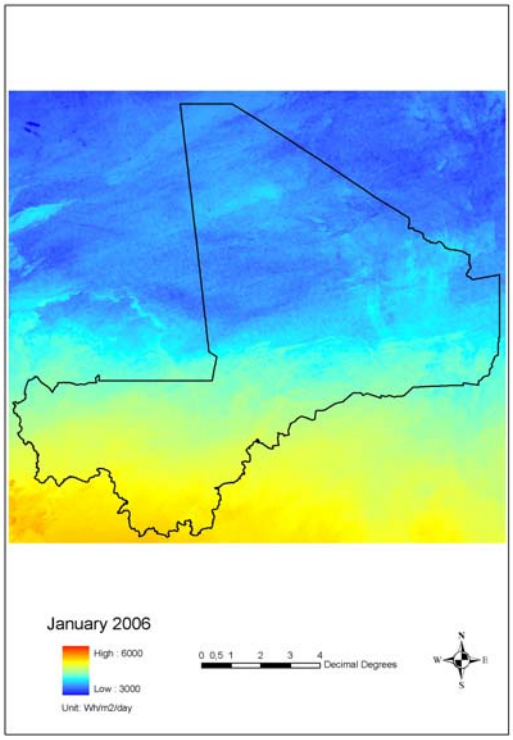


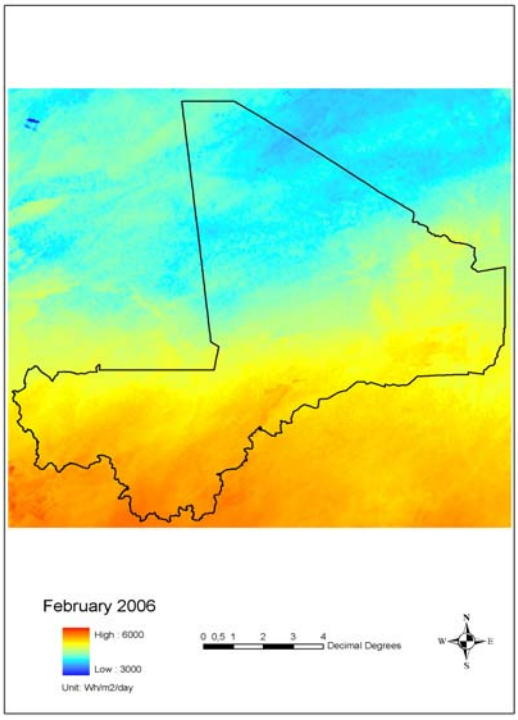


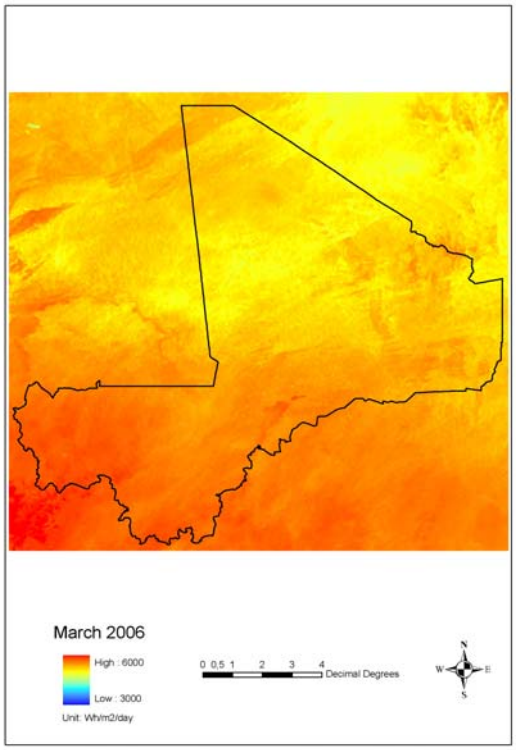


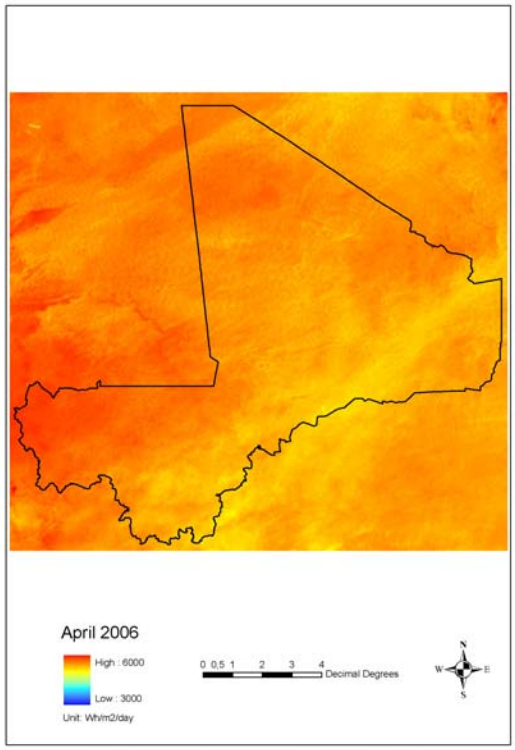

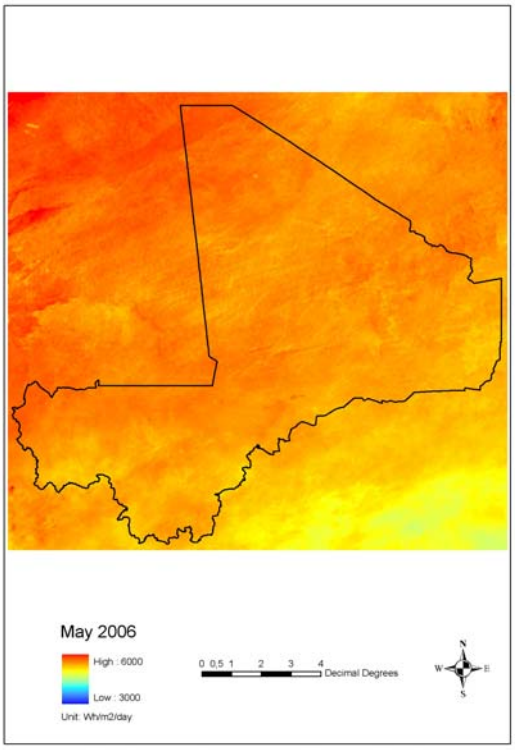
May 2006
High : 6000
Low : 3000
Unit: Wh/m2/day
0 0.5 1 2 3 4
Decimal Degrees
N
W
E
S

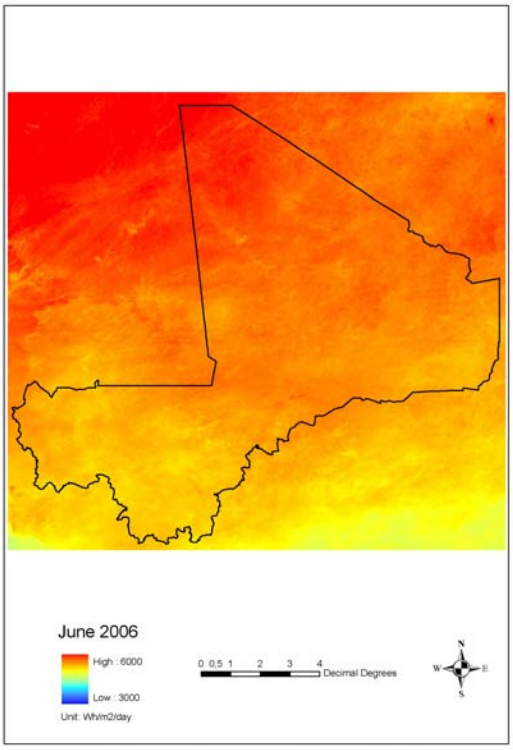
June 2006
High : 6000
Low : 3000
Unit: Wh/m2/day
0 0.5 1 2 3 4
Decimal Degrees
N
W
E
S

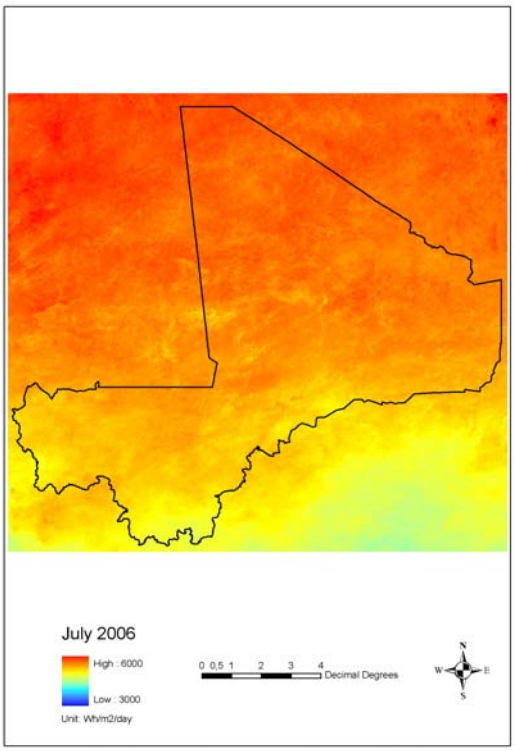
July 2006
High : 6000
Low : 3000
Unit: Wh/m2/day
0 0.5 1 2 3 4
Decimal Degrees
N
W
E
S

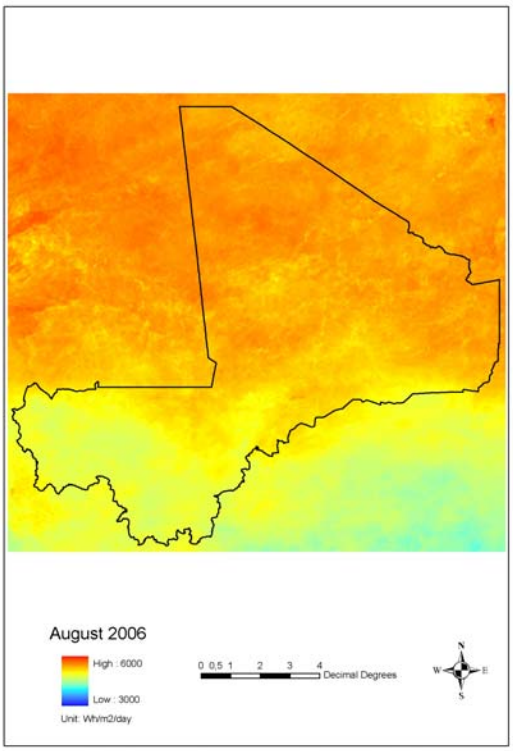
August 2006
High : 6000
Low : 3000
Unit: Wh/m2/day
0 0.5 1 2 3 4
Decimal Degrees
N
W
E
S

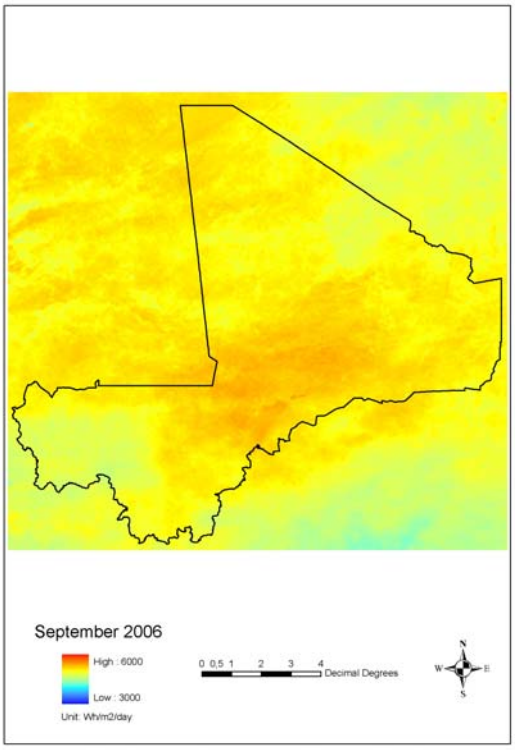
September 2006
High : 6000
Low : 3000
Unit: Wh/m2/day
0 0,5 1 2 3 4
Decimal Degrees
N
W
E
S

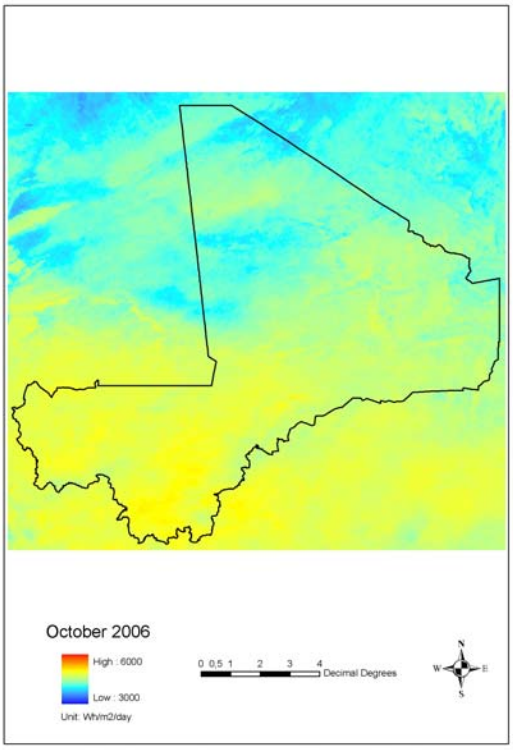
October 2006
High : 6000
Low : 3000
Unit: Wh/m2/day
0 0,5 1 2 3 4
Decimal Degrees
N
W
E
S

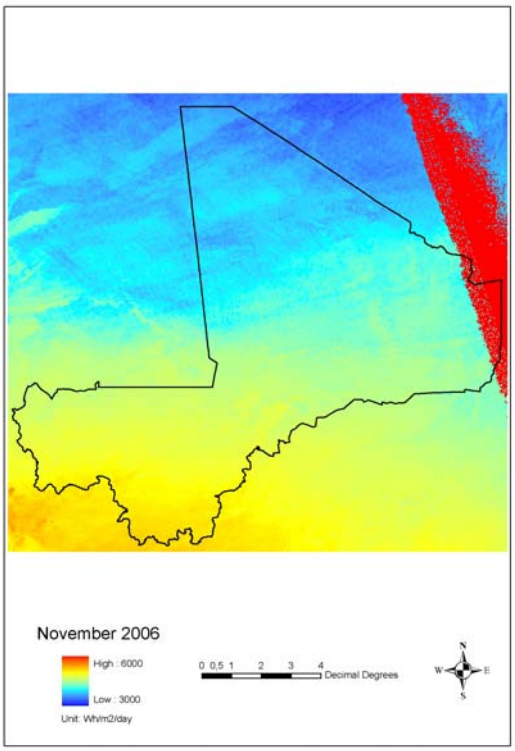
November 2006
High : 6000
Low : 3000
Unit: Wh/m2/day
0 0,5 1 2 3 4
Decimal Degrees
N
W
E
S

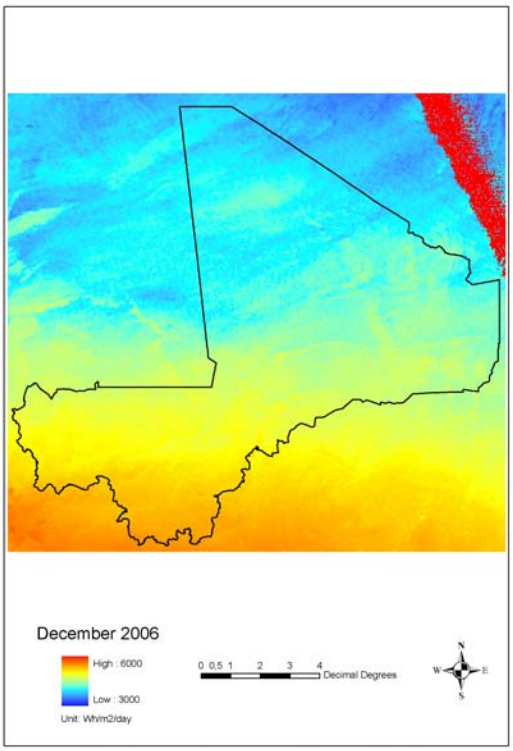
December 2006
High : 6000
Low : 3000
Unit: Wh/m2/day
0 0,5 1 2 3 4
Decimal Degrees
N
W
E
S

**Appendix B :**

# EVALUATION DES RESSOURCES DE LA BIOMASSE AGRICOLE ET DE SA VALORISATION ENERGETIQUE AU MALI

**Par**

**Dr Ibrahim TOGOLA**
**Mali-Folkecenter (MFC)**

**Juin 2008**

# Contenu

# 1 Présentation du Mali


Le Mali est un vaste pays situé au cœur de l'Afrique de l'Ouest. Il s'étend entre le 10ème et 25ème degré de latitude Nord d'une part et d'autre part entre le 4ème degré de longitude Est et le 12ème degré de longitude ouest, sur une superficie de 1.241.231 km2. En 2004, la population du Mali était estimée à 12,5 millions avec plus de 80% de cette population vivant en milieu rural [1].

# 2 Présentation Succincte de la Situation Energétique du Mali

Comme bon nombre de pays africains, la situation énergétique du Mali est caractérisée par :

- Une exploitation excessive des ressources forestière
- Sa grande dépendance des produits pétroliers qui sont totalement importés
- Le coût élevé du développement du potentiel d'énergie renouvelable dont le pays regorge.

En 2002, la consommation énergétique globale du Mali était de 3.212.559 Tonne Equivalent Pétrole (tep). Cette énergie provient principalement de la biomasse (81%), des produits pétroliers (16%), l'électricité (3%) et les énergies renouvelables utilisées à un niveau insignifiant. La consommation des des ménages contribuent à plus de 86% à la consommation totale du Mali et provient essentiellement de la biomasse énergie. Les secteurs du transport de l'industrie et de l'agriculture contribuent respectivement à 10%, 3% et 1% dans le bilan énergétique national [1].

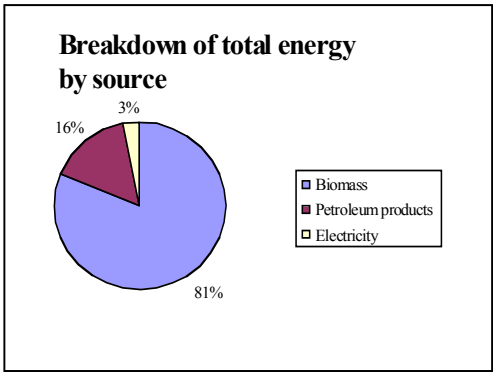


# 3 Disponibilités des Résidus Agricoles au Mali

En tant que pays à vocation agro-pastorale, le Mali dispose chaque année d'importantes quantités de résidus agricoles et agro-industriels. La majeure partie des résidus agricoles est concentrée dans les zones agricoles ou industrielles comme : la zone rizicole de l'Office du Niger, la zone cotonnière de la Compagnie Malienne de Développement du Textile (CMDT), et la zone arachidière de Kita.

## 3.1 Zone Rizicole

### 3.1.1 Balle de riz

Les quantités de balle de riz produite au Mali sont très importantes. Avec une production d'environ 800 000 tonnes/an de riz paddy, le disponible en balle de riz est de 264 000 tonne/an. Ce potentiel peut servir pour la production d'électricité [2].

### 3.1.2 Paille de riz

Selon une estimation du CNESOLER, la production annuelle de paille de riz dans la zone office du Niger s'élèverait à 135 000 tonnes dont la moitié est réservée à

l'alimentation du bétail. L'autre moitié est disponible dans les champs des producteurs et est brûlée lors de la préparation pour les campagnes agricoles. Cette paille pourrait servir pour la production de briquette ou la production de vapeur et d'électricité [3].

### 3.1.3 Typha Australis

Le Mali dispose d'une quantité importante de biomasse provenant du typha australis dans la zone rizicole de l'Office du Niger. Le Typha constitue une sérieuse nuisance pour les aménagements hydrauliques de l'Office du Niger. Le potentiel estimé est de l'ordre de 100 tonnes/ha. D'autres plantes envahissantes comme la jacinthe d'eau et la salvinia molesta sont également disponible sur le fleuve Niger et peuvent être utilisées pour la fabrication de briquettes combustibles [4].

### 3.1.4 Bagasse

Pour les deux sucreries actuellement installées au complexe sucrier du Kala Supérieur SUKALA, la production totale de bagasse est estimée à plus de 360 000 tonnes par an. La superficie actuellement cultivée par SUKALA-SA est de 5 000ha. Pour rendre autosuffisant le pays, le gouvernement malien a créé en novembre 2003, en partenariat avec le Groupe américain Schaffer une société de promotion d'un grand projet sucrier à Markala (centre), appelée Société sucrière de Markala (SOSUMAR). Cette unité occupera une superficie de 18.000 hectares. Sukala-SA a aussi annoncé la construction d'une nouvelle sucrerie de 60.000 à 100.000 tonnes de sucre ce qui nécessitera l'augmentation de la superficie actuellement cultivée en canne à sucre.
Tous ces projets permettront au Mali de disposer d'une quantité importante de bagasse. [5].

## 3.2 Zone cotonière

### 3.2.1 Tiges de coton

Le coton est l'une des principales cultures agricoles du Mali. Dans les zones CMDT, on estime à plus de 500 000 tonnes de tiges de cotonnier produits par an. En considérant un taux de rendement de 20% pour la carbonisation on obtient un équivalent de 100 000 tonnes de poudre qui peut être utilisée pour la production de briquette combustible [2].

### 3.2.2 Tiges de Millet et Sorgho

Dans la zone cotonnière il est également estimé un potentiel de près de 400 000 tonnes de millet et sorgho qui pourrait générer plus de 100 000 tonnes de briquettes de charbon [3].

## 3.3 Zone arachière

La production d'arachide dans la zone de Kita est d'environ 15 millions de tonnes d'arachides [3].

# 4 Possibilité de valorisation énergétique des Résidus agricoles au Mali

Les sous-produits agricoles au Mali sont disponibles en grande quantité. Une faible partie seulement de cette ressource est utilisée à des fins d'aliments bétails, dans le

compostage ou recyclée d'une autre façon. La plupart du temps et malgré les efforts de sensibilisation de divers intervenants aux problèmes écologiques, ces résidus, sont simplement brûlés ou déversés dans la nature. La production de briquette de charbon fabriquée à partir d'une multitude de résidus agricoles peut être une alternative à la coupe du bois.

En effet, les tiges de coton, de mil, de sorgho et de maïs, les coques d'arachide, les pailles et les balles (enveloppe ou son) de riz se sont tous avérés d'excellents combustibles. Les briquettes peuvent êtres constitués d'une seule de ces matières, ou d'un mélange de plusieurs matières. Les tests effectués sur la balle de riz ont été encourageants. La balle de riz fournit une briquette plus solide maïs demande une carbonisation plus lente et plus complexe. Les tests effectués à Bamako ont révélé un rendement de carbonisation de 48% sur les résidus de balle de riz [3]. Le tableau ci-dessous montre la valeur énergétique de briquettes combustibles pour différents résidus agricoles.

**Tableau 1 : Pouvoir énergétique de briquette à base de divers résidus agricoles**

| | Briquettes de tiges de cotonniers | Briquettes de coques d'arachides | Briquettes de tiges carbonisées | Briquettes de bagasse de canne à sucre |
|---|---|---|---|---|
| Pouvoir énergétique en TEP | 0,386 | 0,495 | 0,434 | 0,505 |

Source : [8].

# 5 Actions de valorisation énergétique des résidus agricoles au Mali

La valorisation énergétique des résidus agricoles au Mali est très timide. Quelques actions ont été réalisées dans le cadre de projets et programme mis en œuvre par le gouvernement, les opérateurs privés et les ONG. Parmi ces programmes on peut citer :

## 5.1 Tiges de Cotonnier

- **La production et la commercialisation de briquette combustible à base des résidus des tiges de coton et des résidus de charbon de bois.** Cette action a été réalisée dans le cadre de la stragétgie énergie domestique (SED) qui a été mis en œuvre au Mali entre 1996 et 2002 pour la protection de l'environnement et la lutte contre la désertification. L'une des stratégie de ce projet a été la généralisation de l'utilisation des combustibles alternatifafs aux bois dans toutes les villes du Mali. Dans le cadre de la SED l'entreprise privée (Biommasse-Mali) a recu un appui pour la production et la commercialisation de briquette combustible à base des résidus des tiges de coton et des résidus de charbon de bois. La technique de production utilisée est l'agglomération du poussier de charbon en briquettes. Les tiges de coton sont carbonisées directement dans un carbonisateur dans les champs des paysans pour obtenir du poussier de charbon. Les résidus de charbon sont collectés dans les points de vente du charbon. Une unité de production est installée à Bamako sur la route de Koulikoro. Cette unité a une capacité de production de 600 Kg en huit heures [9].

- **Une étude de faisabilité pour la fabrication de bûches, bûchettes** à partir de tiges de cotonnier a été réalisée. La production théorique annuelle de l'unité de production qui devrait être installé à Fana est de 5 000 tonnes par an. Cette étude a révélé que la production de bûches et bûchettes est économiquement rentable [7].

### 5.2 Utilisation de la balle de riz pour la production d'électricité

L'Office du Niger dispose de trois centrales fonctionnant au gaz pauvre produit à partir de la balle de riz. Ces trois centrales utilisent 3 750 tonnes de balle de riz par an pour la production d'électricité. Chaque centrale est équipée d'un gazogène produisant 780 m3 de gaz pauvre par heure, un moteur à gaz pauvre et un alternateur de 200 kva. Cependant il faut noter que ces installations de fonctionnent plus normalement par manque de pièce de rechange essentiellement [6].

### 5.3 Utilisation de la bagasse

Une infime partie de la bagasse produite dans les sucreries de Dougabougou et Seribala est actuellement utilisée pour la production de vapeur utilisée dans la chaîne technologique et pour produire de l'électricité pour faire tourner l'usine. Le tableau suivant donne la quantité d'électricité qui était produite à partir de la bagasse dans les années 1994.

**Tableau 2 : Production d'électricité à partir de la bagasse**

| | Puissance installée en KW | Heure de fonctionnement /an | Production en Kwh |
|---|---|---|---|
| Dougabougou | 850 | 3 960 | 3 366 000 |
| Séribala | 1 200 | 3 780 | 4 536 000 |
| Total | 2 050 | 7 740 | 7 902 000 |

Source : [6].

### 5.4 Utilisation Typha australis

Dans le cadre du Programme Régional de Promotion des Energies Domestiques et Alternatives au Sahel **(**PREDAS), la valorisation du Typha à des fins de production d'énergie domestique est en voie d'exploration. En Octobre 2003, les premiers tests de production et d'utilisation d'agglo-briquettes de charbon de Typha australis ont été réalisés au Mali par le PREDAS. Ces tests ont donné des résultats très encourageants, qui en démontrent la faisabilité technique dans le contexte sahélien, et les perspectives que cela représente en termes de création d'emploi. Le PREDAS est mis en œuvre dans les pays membres du Comité permanent Inter-états de Lutte contre la Sécheresse au Sahel (CILSS). Les objectifs globaux du PREDAS sont (i) d'aider les Etats membres du CILSS à organiser durablement l'approvisionnement et l'utilisation rationnelle des énergies domestiques des populations sahéliennes, en particulier sans préjudice sur l'environnement et (ii) de contribuer à la lutte contre la pauvreté. Il s'agit plus spécifiquement de créer un cadre favorable à une gestion organisée et durable des ressources en énergies domestiques.

### 5.5 Utilisation de divers résidus

Dans le cadre du volet énergie domestique du projet énergie domestique et accès aux services de base en milieu rural (PEDASB) mis en œuvre par l'Agence Malienne pour le Développement de l'Energie Domestique et l'Electrification (AMADER) la promotion des foyers et fourneaux améliorés utilisant divers résidus est faite par un opérateur privée. Cet type de foyer amélioré est connu sous le nom de « Taré Taré ».

# 6 Conclusion

Le Mali dispose d'un important potentiel de résidus agricoles qui reste jusqu'à présent timidement valorisé à des fins énergétiques. Pour assurer une gestion efficace de la biomasse-énergie, la nouvelle approche des autorités maliennes vise à établir un partenariat basé sur la compréhension et le respect mutuel par la concertation et par les rapports contractuels entre les acteurs (Etat, ONG, Ruraux, Collectivités) engagés conjointement dans les différentes actions d'aménagement forestier, de transformation et de distribution de la biomasse-énergie sous ses différentes formes. C'est ainsi que l'état malien met en œuvre des mesures incitatives d'ordre économique et financières (exonération sur les différents équipements) pour encourager les différents opérateurs à la valorisation des résidus agro-industriels par leur transformation.

## Bibliographie


(1) Politique énergétique du Mali, 2004
(2) Énergie et écodéveloppement au Mali, Cheick Ahmed Sanogo, 2005 (www.helio-international.org/reports/pdfs/Mali-FR.pdf)
(3) Potentialités de la biomasse au Mali, Aminata Fofana
(4) www.aurythmedelafrique.org/3**mali**/paysvuparnous_**mali**.htm
(5) CDM Project Idea Note developped for Sukala-SA, 2006
(6) Rapport du projet 'Regional Programme for Traditional Energy Strategy' (RPTES), Banque Mondiale,1994
(7) Rapport de l'étude de faisabilité d'un projet de fabrique de bûchettes et bûches à Fana, Mars 1994
(8) Document de vision et de stratégie régionale de valorisation énergétique de la biommasse pour un développement durable UEMOA
(9) Catalogue of energy intervention in Mali, DEA project, 2005